STUDIES OF COMPOUND STATES OF NEGATIVE IONS USING LASER BEAMS*

Office of Naval Research Task NR 393-071

R. N. Compton and G. D. Alton

Oak Ridge National Laboratory
Oak Ridge, Tennessee 37831

August 1985

*Research sponsored by the Office of Naval Research under Interagency Agreement Number 40-1147-81. Oak Ridge National Laboratory is operated by Martin Marietta Energy Systems, Inc., with the U.S. Department of Energy under contract DE-AC05-84OR21400.

SECURITY CLASSIFICATION OF THIS PAGE

REPORT DOCUMENTATION PAGE

1a REPORT SECURITY CLASSIFICATION	1b RESTRICTIVE MARKINGS
2a SECURITY CLASSIFICATION AUTHORITY	3 DISTRIBUTION / AVAILABILITY OF REPORT Approved for public release; distribution unlimited.
2b DECLASSIFICATION / DOWNGRADING SCHEDULE	
4 PERFORMING ORGANIZATION REPORT NUMBER(S) DOE 40-1147-81	5 MONITORING ORGANIZATION REPORT NUMBER(S) N/A
6a NAME OF PERFORMING ORGANIZATION Oak Ridge National Laboratory 6b OFFICE SYMBOL (If applicable)	7a NAME OF MONITORING ORGANIZATION N/A
6c ADDRESS (City, State, and ZIP Code) P.O. Box X Oak Ridge, Tennessee 37831	7b ADDRESS (City, State, and ZIP Code) N/A
8a NAME OF FUNDING / SPONSORING ORGANIZATION Office of Naval Research 8b OFFICE SYMBOL (If applicable)	9 PROCUREMENT INSTRUMENT IDENTIFICATION NUMBER N00014-85-F-0011
8c ADDRESS (City, State, and ZIP Code) Physics Division, Code 421 800 North Quincy Street Arlington, Virginia 22217	10 SOURCE OF FUNDING NUMBERS PROGRAM ELEMENT NO: 61153N PROJECT NO: RR 011-03[illegible] TASK NO: NR393-071 WORK UNIT ACCESSION NO:

11 TITLE (Include Security Classification)
Studies of Compound States of Negative Ions Using Laser Beams

12 PERSONAL AUTHOR(S)
R. N. Compton and G. D. Alton

13a TYPE OF REPORT	13b TIME COVERED	14 DATE OF REPORT (Year, Month, Day)	15 PAGE COUNT
Summary	FROM 10/12/84 TO 9/30/85	August 15, 1985	

16 SUPPLEMENTARY NOTATION Prepared in cooperation with Dr. D. J. Pegg and J. S. Thompson (University of Tennessee), T. J. Kvale (ORAU Postdoctoral Fellow) A. Dodhy (Graduate Student, Auburn)

17 COSATI CODES		
FIELD	GROUP	SUB-GROUP

18 SUBJECT TERMS (Continue on reverse if necessary and identify by block number)
Laser photodetachment of negative ion beams; Neutralization of negative ion beams; Autodetachment spectroscopy of negative ion beams; Electron collisions in strong laser fields

19 ABSTRACT (Continue on reverse if necessary and identify by block number)
This research involves experimental studies of compound states of negative ions using laser beams. Negative ion beams of stable (H^-, O^-, etc.) and metastable (He^-, Be^-, Ca^-, etc.) species are generated by double charge exchange from positive ion beams colliding with alkali vapor. Measurements of the photodetachment and autodetachment spectra for these ions provide new information on compound state energy levels. In addition experiments are underway to study the collisions of electrons with atoms in strong laser fields. Many theoretical predictions have been presented recently on this subject. These experiments should provide the first tests of such predictions.

20 DISTRIBUTION / AVAILABILITY OF ABSTRACT	21 ABSTRACT SECURITY CLASSIFICATION
☒ UNCLASSIFIED/UNLIMITED ☐ SAME AS RPT ☐ DTIC USERS	
22a NAME OF RESPONSIBLE INDIVIDUAL R. N. Compton	22b TELEPHONE (Include Area Code) 615/574-6233
	22c OFFICE SYMBOL

DD FORM 1473, 84 MAR 83 APR edition may be used until exhausted. All other editions are obsolete

SECURITY CLASSIFICATION OF THIS PAGE

STUDIES OF COMPOUND STATES OF NEGATIVE IONS USING LASER BEAMS

R. N. Compton and G. D. Alton

Oak Ridge National Laboratory, Oak Ridge, Tennessee 37831

This is a second-year progress report and third-year proposal on our research effort entitled "Studies of Compound States of Negative Ions Using Laser Beams" under Office of Naval Research (ONR) task NR 393-071. The reader will note a change in the title of the proposal from that of the previous year, namely, "... Atomic Negative Ions" is replaced by "... Negative Ions" in order to reflect the new work we will describe on molecular negative ions (He_2^-). Our proposed and completed research effort can be separated into two well-defined activities: (I) Autodetachment, Collisional Detachment, and Photodetachment Studies of H^-, He^-, Be^-, Ca^-, and He_2^- and (II) Experimental Studies of Electron Collisions in the Field of a Laser. Two *Physical Review* and one *Physical Review Letters* articles have been published. One article describing studies of Ca^- production has been accepted by *Nuclear Instrumentation and Methods*, and *Physical Review Letters* has accepted our manuscript entitled "Experimental Determination of the Energy Level of Be^- $(1s^22s2p^2)^4P$." A third *Physical Review Letters* article entitled "Autodetachment Spectroscopy of He_2^-" is in final preparation and will be submitted soon. All of these articles are included as Appendix I.

The Office of Naval Research support has allowed the researchers to develop this program into an important basic research component at the Oak Ridge National Laboratory. The group consists of R. N. Compton (Health and Safety Research Division) and G. D. Alton (Physics Division), Oak Ridge National Laboratory, D. J. Pegg, professor of physics, The University of Tennessee, and most importantly, T. J. Kvale, postdoctoral fellow from The University of Missouri-Rolla. Dr. Pegg has

separate support from the Department of Energy (Basic Energy Sciences) which also supports J. S. Thompson, a full-time graduate student from The University of Tennessee. The Negative Ion Source Test Facility has been primarily funded by the Physics Division. ONR funds mainly pay for the support of Dr. T. J. Kvale and some of the day-to-day operational expenses. Dr. Kvale has mastered the experimental complexities of the Negative Source Ion Test Facility. Three other graduate students have been associated with the project in various capacities and are responsible for the day-to-day operation of the facility and much of the data acquisition and analysis. Adila Dodhy, a graduate student from Auburn University, has been studying laser-induced "continuum-continuum" effects under high laser fields. Her Ph.D. thesis is now complete and she will be joining Dr. H. Walther's group at the Max Planck Institute in Garching, West Germany in September 1985. Michael Shea, graduate student in physics at Vanderbilt University, contributed to the development of a laser produced, high resolution, high emittance electron beam.

The past year has been very productive; the Negative Ion Source Test Facility and the laser experiments have operated continuously. Therefore, there are a number of results to report, and we will describe only final results, referring the reader to the papers in Appendix I for details.

We will separate discussions of the progress into two parts. Part I will summarize the studies of negative ion states of Ca^-, Be^-, and He_2^-. Part II will describe results and progress on high laser field effects on electron-atom collisions. In Part III, we will present our proposed direction of research. The proposal is strongly influenced by a recent study of He_2^- to be described in Part I below.

I. Studies of Negative Ions

The new, modified Negative Ion Source Test Facility is now operating routinely. This major apparatus was described in detail in the previous progress report and to a lesser extent in the papers enclosed in Appendix I. However, further improvements to

the facility will be made by installation of a recently procured 200 kV, 10 mA highly regulated power supply. This will give us the capability of producing and studying heavy negative ions such as Ca^-. Progress during the early portion of this fiscal year was inhibited by severe reliability problems with the commercially procured hollow cathode positive ion source which made spectroscopic measurements of the type discussed in this report difficult, if not impossible. The severe nature of the problem necessitated a complete redesign and development of a new or more reliable source. The source has been fabricated, tested, and utilized in the Be^- and He_2^- spectroscopic investigations. The success of these experiments is largely attributable to this development. This development constitutes a major improvement to the technology of hollow cathode positive ion sources. The sources will be the subject of a forthcoming report which will be submitted for publication in RIS or *Nuclear Instrumentations and Methods.* Operation of the ion source with beryllium also required special handling procedures and sometimes made progress cumbersome and oftentimes slow, however, we have successfully completed the Be^- studies as described below.

We have completed measurement of the energy level of $Be^-(1s^22s2p^2)^4P$. Details of these measurements are to be found in Appendix I. Be^- ions were produced in sequential charge exchange collision between 50- and 60-keV Be^+ ions and lithium vapor. The energy level of Be^- was determined directly by measuring the autodetached electron energies leaving the atom in the ground state. Figure 1 shows one such measurement. The electron energy scale was calibrated using the collisional "cusp" peak at $\sim$3.5 eV. There is an approximately three to one compression of the lab to center-of-mass energy, thus, the electron energy resolution can be seen to be $\sim$50 meV. Our experimental value is compared with four theoretical values in Table I. This represents the first experimental measurement of the energy level of a metastable negative ion of the Group II metals. Previous to this measurement only one other metastable energy level, that of $He^-(^4P)$, had been reported.[1]

We have begun measurements on the energy levels for metastable states of other Group IIA metals, Mg^- and Ca^-. In this connection, we have determined production efficiencies for Ca^-. These results are described in the preprint found in Appendix I.

We have also completed and reported studies of collisional detachment of H^- ions with various target gases. Again these results are described in the preprint contained in Appendix I. This paper represents only the second such study of collisionally detached "cusp" electron spectroscopy for a negative ion. These studies have relevance to neutral beam technology.

Perhaps the most interesting results to date are the recent measurements on He_2^-. Long-lived metastable negative ion beams of He_2^- have been recently produced for the first time by Bae, Coggiola, and Peterson.[2] The electronic structure of He_2^- has been subsequently investigated by Michels[3] who finds the $^4\Pi_g$ $(1s\sigma_g^3 1s\sigma_u 2s\sigma_g^2 p\Pi_u)$ state of He_2^- to be bound relative to the lowest triplet state He_2^* $(a^3\Sigma_u^+)$ by 0.233 eV. These theoretical studies further show that the $^4\Sigma_g^+$ $(1s\sigma_g^2 1s\sigma_u 2\sigma_y 2s\sigma_u)$ negative ion state is unbound relative to He_2^* $(a^3\Sigma_u^+)$ for internuclear separation $\leqslant 6$ Å. For internuclear separations near the potenital minimum ($\sim$1 Å), the $^4\Sigma_u^+$ state tracks sufficiently close to the $a^3\Sigma_u^+$ state that it was not possible to determine whether this state is stable. More extensive calculations of this potential are in progress (H. H. Michels, private communication). We have recently begun a study of electron autodetachment spectroscopy of metastable He_2^- formed by double charge exchange of energetic (30-65 keV) He_2^+ ions with lithium vapor. Figure 2 shows a typical electron spectrum covering the range from 0 to 50 eV in the laboratory system. The steep rise at $\sim$0 eV is due to secondary electrons from ion and electron scattering with slits, etc. which defines the path of the ion beam. The peaks at $\sim$2 and 33 eV are due to autodetachment from He_2^-. The peak at $\sim$2 eV can be resolved into two peaks and will be discussed below. The peak at 33 eV results from autodetachment from He_2^- $(^4\Pi_g)_{v=0}$ to 2He (^1S) + e as illustrated in Fig. 3. Using the vibrational

wavefunctions from the calculations of Michels[3] and the average of a large number of data as shown in Fig. 2, we have constructed a potential energy function for two ground state helium atoms interacting at ~1 Å. There are numerous theoretical and experimental estimates for this potential function (see Foreman, Roland, and Coffin[4]) all of which differ by more than 1.5 eV. Our preliminary measurements favor the lower of all of these potentials.

Figure 3 shows a high-resolution scan of the low-energy two peaks for various $^4He_2^-$ ion energies. The kinematic shifts clearly show that the two peaks which result from forward and backward electron ejection in the center-of-mass system corresponding to 11.4 meV autodetachment energy. The potential energy function for He_2^- ($^4\Pi$) is approximately congruent with that of He_2^* ($a^3\Sigma_u^+$) and shifted down by approximately 0.223 ± 0.030 eV according to the calculations of Michels.[3] As a result, vibrational autodetachment of excited He_2^- is expected to follow the propensity rule $\Delta v = 1$ and $\Delta J = 0$. Therefore, except for the small anharmonicities (which are too small to detect at the present level of resolution), single, narrow peaks are expected for both ejected electron directions, as shown in Fig. 3. Figure 4 shows the same spectra for the isotopic species $^3He_2^-$. The autodetachment peak shifts up to 40 meV in the center-of-mass frame. Again neglecting small anharmonicities, the difference between the autodetached electron energy for $^3He_2^-$ and $^4He_2^-$ would be given by $3/2(\hbar\nu_3^- - \hbar\nu_4^-) - 1/2(\hbar\nu_4^0 - \hbar\nu_3^0)$ where ν_3^0 and ν_4^0 represents the frequencies for $^3He_3^0$ and $^4He_4^0$, respectively. Using the measured difference of 37.4 - 11.4 = 26 meV and known values for $\hbar\nu_3^0$ and $\hbar\nu_4^0$, we calculate a vibrational energy of 0.22 eV for $^3He_3^-$ and 0.019 for $^4He_4^-$ which is close to that calculated by Michels. As expected, the negative ion frequencies are very close to those of the corresponding $a^3\Sigma_u^+$ state. Assuming that these peaks represent vibrational autodetachment from $v = 1$ of the ion to $v = 0$ of the neutral, we calculate an electron affinity for $^4He_2^*$ of 0.18 eV which is ~ 0.05 eV lower than the theoretical value of Michels who, in fact, computes the first vibrational level of He_2 ($^4\Pi$) to be

bound. The discrepancy is within the theoretical uncertainty of the calculations. On the other hand, we cannot rule out the possibility that the peaks in Figs. 2 and 3 are vibrationally autodetached from the $^4He_2^-$ ($^4\Sigma_u^+$) state provided that this ion is bound. Further comparison awaits more detailed calculations.

The present results show that He_2^- is formed by adding an extra electron to the first excited triplet $a^3\Sigma_u^+$ state of He_2. Furthermore, isotopic studies provided a vibrational energy for the $v=1$ to $v=0$ state as 0.19 eV. Direct autodetachment to the underlying continuum He(^{1}S) + He(^{1}S) + e provides new information on the classic quantum chemistry problem of two interacting ground state helium atoms. More importantly, these results establish this technique as a powerful method for studying autodetachment processes in metastable molecular negative ions. A manuscript has been prepared for submission to *Physical Review Letters* describing the technique and experimental results for He_2^-. A reprint is contained in Appendix I.

II. Electron Collision in a Strong Laser Field

In our original proposal, we described a set of experiments involving laser-induced transitions between compound negative ion states. Two experiments have been constructed and are generated with these goals in mind. Perry Blazewicz, a graduate student from Yale University, is conducting one of these experiments and some progress has occurred in the development of a laser produced, high resolution, high emittance electron beam. These two projects and their goals were outlined in last year's report. Since that time the subject of "continuum-continuum" absorption or above threshold ionization (ATI) in high intensity MPI experiments have emerged. All of these studies were previously performed for eleven or more photon ionization of xenon. During the course of our studies of two-photon ionization of alkali atom, we observed the "continuum-continuum" electrons and diverted our effort to their study. Adila Dodhy performed this work as part of her Ph.D. dissertation. These studies are presented in Appendix I and will not be discussed further here. A second paper on

angular distributions for above threshold electrons in rubidium has been prepared for publication in *Physical Review Letters* and is also attached to Appendix I.

The studies of strong laser field effects on electron scattering have been a minor component of the ONR studies. However, now that the Negative Ion Source Test Facility is more routine in its operation, greater effort will be devoted in this direction in the coming year. For example, Dr. T. J. Kvale will be free to assist in some of these experiments in the coming year.

III. Proposed Research

The Negative Ion Source Test Facility is now routinely producing results. The studies of Be^- and He_2^- are now complete. The Be^- studies have been published. The studies of He_2^- have illustrated the tremendous utility of this new technique. It is possible to now study autodetachment processes with resolution approaching 1 meV. In essence, we are sitting on a "gold mine" of new and unique research. Our plans are to study the following systems.

Atomic negative ions

1. A search will be conducted for the lowest shape resonance for $Be^-(1s^22s^22p)$. There is considerable theoretical interest in this species. Production of $Be^-(1s^22s^22p)$ will be attempted from double charge exchange between Be^+ and lithium vapor. A new alkali charge exchange cell has been constructed which will allow the electron spectrometer to exist very close to the exit thus permitting the observation of short-lived ions. Unlike the $Be^-(1s^2s2p^2)$ state, the lifetime of $Be^-(1s^22s^22p)$ is expected to be rather short.
2. Metastable energy levels of Mg^- and Ca^- similar to that for Be^- and He^- will be determined. These experiments will be undertaken after performing the Be^- studies.

3. Measurement of the metastable energy level for Ar^- will be considered.

4. We will begin studies of laser photodetachment with electron energy analysis of Be^-, Mg^-, Ca^-, and Ar^-.

Molecular negative ions

1. HeN_e^-, $HeAr^-$, and $HeXe^-$: A search will be conducted for metastable negative ions of mixed He^- rare gas dimer negative ion states. Autodetachment spectroscopy studies of these species will provide new information on the electron affinities and vibrational frequencies for these negative ions, if they exist, as well as potential energy functions for the ground state atoms.

2. H_2O^-: Water is expected to weakly bind an extra electron due to the permanent dipole moment. If this ion is observed, studies of autodetaching electrons may provide new spectroscopic information on H_2O^-.

3. $H_2^-H_3^-$: Metastable states of H_2^- may exist as a result of binding an $H^-(2p^2)^2P^e$ with H(1s). This state of H_2^- could be analogous to He_2^-. H_3^- on the other hand has the structure $H^- \cdot H^+ \cdot H^-$ and is also expected to be unstable. We will search for this ion at the same time studies of H_2^- are conducted.

4. HeH^-: Metastable states of HeH^- and HeD^- are expected to exist as a result of binding $He^-(^4P)$ with H(1s) or $H^-(2p^2)^2P$ with $He(1s^2)$. Isotope shifts using deuterium substitution will provide direct information on the energy level of HeH^-. There is the possibility that HeH^- also has a bound state. If these experiments are successful we will examine NeH^-, ArH^-, and XeH^-. These experiments should be very interesting since large beams of rare gas hybrid positive ions are possible as a result of ion molecular reaction, e.g., $Ar^+ + H_2 \rightarrow ArH^+ + A$.

Monoenergetic Electron Source Using Autodetachment from Metastable Be^-

A simple apparatus has been constructed that should allow ultrahigh (<1 meV) resolution electron spectroscopy studies. The method utilizes that fact that $Be^-(1s^2 2s 2p^2)$ negative ions are metastable and eject monoenergetic electrons. In this connection we have constructed a simple gas cell in order to study electron transmission spectroscopy in the rare gases as a diagnostic test of the method. This is a minor, but perhaps important, deviation from our studies of metastable negative ions.

This represents only a partial list of experiments we plan for the coming year. Parallel to these efforts J. S. Thompson has been designing an apparatus which will allow photodetchment studies of the negative ion beam discussed above. His studies will be similar to our earlier studies[5] of photodetachment of He^- where total detachment cross sections were determined. This work along with the autodetachment studies will constitute his Ph.D. dissertation.

During the coming year we will continue our progress on studies of electron collisions in a laser field. Dr. T. J. Kvale will devote part of his time to these experiments. This should hasten progress in this area considerably. The basic experiments which are underway have been described in the previous proposal and will not be restated here. In addition to these experiments during the past year, there has been considerable interest in the so-called "above threshold ionization" (ATI) spectroscopy or "continuum-continuum" scattering. We have added new information to this exciting field (see Appendix I). Our studies were limited to alkali atoms using laser power densities of $\sim 10^{11}$ W/cm^2. Recently, there has appeared studies on xenon atoms by the Dutch group headed by M. Van der Weil and a French group headed by G. Mainfray. These results are somewhat in discord with regards to the ATI data. We intend to repeat these measurements and also the measure the angular distributions for the ATI electrons.

References

1. See G. D. Alton, R. N. Compton, and D. J. Pegg, *Phys. Rev.A* **28**, 1405 (1983) and other cited therein.

2. Y. K. Bae, M. J. Coggiola, and J. R. Peterson, *Phys. Rev. Lett.* **52**, 747 (1984).

3. H. H. Michels, *Phys. Rev. Lett.* **52**, 1413 (1984).

4. P. B. Foreman, P. K. Roland, and K. P. Coffin, *J. Chem. Phys.* **61**, 1658 (1974).

5. R. N. Compton, G. D. Alton, and D. J. Pegg, *J. Phys. B* **13**, L651 (1980).

Table 1. Summary of experimental and theoretical values for the energy levels of the $Be^-(1s^22s2p^2)^4P$ state

Electron affinity $E[Be(^3P) - Be^-(^4P)]$ (meV)	State energy $E[Be^-(^4P)]$ (eV)	Type	Reference
240 ± 100	2.49[a]	Theoretical	1
>122	2.66[b]	Theoretical	2
285		Theoretical	3
217.7 ± 57.1	2.56[c]	Theoretical	4
195 ± 90[d]	2.53 ± 0.09	Experimental	Present work

[a]used −14.6189 a.u. for the ground state of beryllium.

[b]used −14.6684 a.u. for the ground state of beryllium as quoted from Ref. 5.

[c]used −14.667328 a.u. for the ground state energy of beryllium as quoted from Ref. 5.

[d]used 2.7248 eV as the state energy of $Be(1s^22s2p)^3P^0$ taken from Ref. 6.

Budget

A. Support for Personnel (Including Fringe Benefits and Overhead)

	1985	1986
R. N. Compton(5%)	$10,000	$12,000
G. D. Alton (5%)	10,000	12,000
Postdoctoral Fellow	41,000	41,000

B. Ancillary Cost

Technical Support	6,000	6,000
Travel	1,000	1,000
Channeltron Detector	1,000	1,000
Publication and Supplies	1,000	1,000
TOTAL	70,000	74,000

APPENDIX I

RESUME

NAME: Thomas Jay Kvale

PII Redacted [redacted]

TITLE: Postdoctoral Fellow in Physics

[redacted]

[redacted]

EDUCATION:

A.B.	Gustavus Adolphus College (Cum Laude), 1975
M.S.	University of Missouri-Rolla, 1977
Ph.D.	University of Missouri-Rolla, 1984

ACADEMIC AND PROFESSIONAL EXPERIENCE:

1974-1975	Academic Assistant, Gustavus Adolphus College
1975-1977	Graduate Teaching Assistant, University of Missouri-Rolla
1977-1983	Graduate Research Assistant, University of Missouri-Rolla
1984-Present	Postdoctoral Research Fellowship with Oak Ridge Associated Universities at the Oak Ridge National Laboratory

Ph.D. DISSERTATION TITLE:

Angular Differential Cross Sections for the Excitation of 1^1S Helium to the 2^1S and 2^1P States by 25- to 100-keV Proton Impact

PROFESSIONAL AFFILIATIONS:

American Physical Society, Division of Atomic, Molecular, and Optical Physics
Sigma Xi

HOBBIES

Microcomputers/Electronics
Metal Machining
Woodworking
Photography

REFEREED PAPERS

1. J. E. Aldag, J. L. Peacher, P. J. Martin, V. C Sutcliffe, J. George, E. Redd, T. J. Kvale, D. M. Blankenship, and J. T. Park, "Angular Differential and Total Cross Sections for the Excitation of Atomic Hydrogen to Its n=2 State by Helium Ions," *Phys. Rev. A* **23**, 1062 (1981).

2. P. J. Martin, K. Arnett, D. M. Blankenship, T. J. Kvale, J. L. Peacher, E. Redd, V. C. Sutcliffe, C. D. Lin, J. H. McGuire, and J. T. Park, "Differential Cross Sections for Electron Capture from Helium by 25- to 100-keV Incident Protons," *Phys. Rev. A* **23**, 2858 (1981).

3. P. J. Martin, D. M. Blankenship, T. J. Kvale, E. Redd, J. L. Peacher, and J. T. Park, "Electron Capture at Very Small Scattering Angles from Atomic Hydrogen by 25 - 125-keV Protons," *Phys. Rev. A* **23**, 3357 (1981).

4. J. L. Peacher, T. J. Kvale, E. Redd, P. J. Martin, D. M. Blankenship, E. Rille, V. C. Sutcliffe, and J. T. Park, "Elastic Differential Cross Sections for Small-Angle Scattering of 25-, 50-, and 100-keV Protons by Helium Atoms," *Phys. Rev. A* **26**, 2476 (1982).

5. E. Rille, R. E. Olson, J. L. Peacher, D. M. Blankenship, T. J. Kvale, E. Redd, and J. T. Park, "Isotope Effect in Electron-Capture Differential Cross Sections at Intermediate Energies," *Phys. Rev. Lett.* **49**, 1819 (1982).

6. E. Rille, J. L. Peacher, T. J. Kvale, E. Redd, D. M. Blankenship, and J. T. Park, "Momentum Transfer Scaling in Hydrogen-Isotope Collision Systems," *Phys. Rev. A* **27**, 3369 (1983).

7. E. Rille, J. L. Peacher, D. G. Seely, T. J. Kvale, E. Redd, D. M. Blankenship, and J. T. Park, "Isotope Effect and Momentum-Transfer Scaling in the Elastic-Scattering Differential Cross Sections for Hydrogen-Isotope Collision Systems," *Phys. Rev. A* **28**, 3642 (1983).

8. J. T. Park, E. Redd, T. J. Kvale, and E. Rille, "Reactive Scattering Cell for Atomic Hydrogen and Deuterium," *Rev. Sci. Instrum.* **54**, 1247 (1983).

9. J. L. Peacher, P. J. Martin, D. G. Seely, J. E. Aldag, T. J. Kvale, E. Redd, D. M. Blankenship, V. C. Sutcliffe, and J. T. Park, "Angular Differential and Total Cross Sections for the Excitation of Atomic Hydrogen to Its n=2 Level by 25-150 Hydrogen Molecular Ions," *Phys. Rev. A* **30**, 729 (1984).

10. T. J. Kvale, D. G. Seely, D. M. Blankenship, E. Redd, T. J. Gay, M. Kimura, E. Rille, J. L. Peacher, and J. T. Park, "Angular Differential Cross Sections for the Excitation of 1^1S Helium to the 2^1S and 2^1P States by 25− to 100−keV Proton Impact," *Phys. Rev. A* **32** (1985).

11. T. J. Kvale, G. D. Alton, R. N. Compton, D. J. Pegg, and J. S. Thompson, "An Experimental Determination of the Energy Level of $Be^-(1s^22s2p^2)^4P_J$," *Phys. Rev. Lett.* **55**, 484 (1985).

12. G. D. Alton, T. J. Kvale, R. N. Compton, D. J. Pegg, and J. S. Thompson, "The Production of Ca^- Through Sequential Charge Exchange with Li Vapor," *Nucl. Instrum. Methods* (submitted for publication).

13. T. J. Kvale, R. N. Compton, G. D. Alton, J. S. Thompson, and D. J. Pegg, "Autodetachment Spectroscopy of Metastable He_2^-," *Phys. Rev. Lett.* (to be submitted for publication).

NONREFEREED PAPERS

1. P. J. Martin, J. E. Aldag, T. J. Kvale, J. L. Peacher, E. Redd, V. C. Sutcliffe, and J. T. Park, "Differential Excitation Cross Section Measurements of Atomic Hydrogen to the n=2 State by 25 to 150 keV Hydrogen Molecular Ion Impact," *Bull. Am. Phys. Soc.* **23**, 1087 (1978).

2. J. E. Aldag, J. M. George, T. J. Kvale, P. J. Martin, J. L. Peacher, V. C.Sutcliffe, and J. T. Park, "Excitation of Atomic Hydrogen to the n=2 State by 15 - 175 keV Helium Ion Impact," *Bull. Am. Phys. Soc.* **23**, 1087 (1978).

3. P. J. Martin, T. J. Kvale, J. L. Peacher, E. Redd, V. C. Sutcliffe, and J. T. Park, "Differential Cross Sections for Electron Capture from Helium by 50 keV Protons," *Bull. Am. Phys. Soc.* **24**, 1187 (1979).

4. T. J. Kvale, J. L. Peacher, E. Redd, P. J. Martin, D. M. Blankenship, V. C. Sutcliffe, and J. T. Park, "Differential Elastic Scattering Cross Sections for 25, 50, and 100 keV Protons Incident on Helium," *Bull. Am. Phys. Soc.* **25**, 1116 (1980). (Presented conference talk)

5. E. Redd, J. L. Peacher, T. J. Kvale, P. J. Martin, D. M. Blankenship, and J. T. Park, "Structure in the Differential Cross Section for Excitation of Atomic Hydrogen to the n=2 State by N^+ with a Velocity of 0.25 a.u.," *Bull. Am. Phys. Soc.* **25**, 1116 (1980).

6. P. J. Martin, T. J. Kvale, J. L. Peacher, E. Redd, D. M. Blankenship, K. Arnett, and J. T. Park, "Differential Cross Sections for Electron Capture in Proton-Hydrogen Atom Collisions," *Bull. Am. Phys. Soc.* **25**, 1135 (1980).

7. J. L. Peacher, D. M. Blankenship, T. J. Kvale, E. Redd, P. J. Martin,and J. T. Park, "Differential Elastic Scattering Cross Sections for Sodium Ions Incident on Atomic Hydrogen for keV Energies," **Proceedings of XII International Conference on the Physics of Electronic and Atomic Collisions** (Abstracts of Contributed Papers, Sheldon Datz, Ed.), Vol. 1, pp. 524-525 (1981).

8. P. J. Martin, D. M. Blankenship, T. J. Kvale, E. Redd, J. L. Peacher, and J. T. Park, "Projectile Structure Effects in Electron Capture at Very Small Scattering Angles for $(1s^22s^22p^n)^+$ + H(1s) Collisions at 55.6 keV," **Proceedings of XII International Conference on the Physics of Electronic and Atomic Collisions** (Abstracts of Contributed Papers, Sheldon Datz, Ed.), Vol. 2, pp. 659-660 (1981).

9. T. J. Kvale, E. Redd, D. M. Blankenship, P. J. Martin, J. L. Peacher, and J. T. Park, "Angular Differential Cross Sections for Neon and Sodium Ion Impact Excitation of Atomic Hydrogen at an Impact Velocity of 1/3 a.u.," **Proceedings of XII International Conference on the Physics of Electronic and Atomic Collisions** (Abstracts of Contributed Papers, Sheldon Datz, Ed.), Vol. 2, pp. 750-751 (1981). (Presented conference poster).

10. J. L. Park, E. Redd, T. J. Kvale, D. M. Blankenship, P. J. Martin, and J. L. Peacher, "Angular Differential Cross Sections for Lithium Ion Impact Excitation of Atomic Hydrogen to the n=2 State at a Relative Velocity of v = 1/2 a.u.," *Bull. Am. Phys. Soc.* **26**, 1306 (1981).

11. T. J. Kvale, J. L. Peacher, E. Redd, E. Rille, D. M. Blankenship, and J. T. Park, "Momentum Transfer Dependence in the Proton-Helium Collision System from 25- to 100-keV," *Bull. Am. Phys. Soc.* **28**, 815 (1983). (Presented conference talk)

12. E. Rille, J. L. Peacher, D. M. Blankenship, T. J. Kvale, E. Redd, and J. T. Park, "Differential Cross Sections of Hydrogen Isotopes at Small Scattering Angles," *Bull Am. Phys. Soc.* **28**, 797 (1983).

13. J. L. Peacher, D. G. Seely, T. J. Kvale, E. Redd, D. M. Blankenship, and J. T. Park, "Excitation of Hydrogen to Its n=2 Level by H_2^+ in the Glauber Approximation," *Bull. Am. Phys. Soc.* **28**, 803 (1983).

14. E. Rille, J. L. Peacher, D. M. Blankenship, T. J. Kvale, E. Redd, and J. T. Park, "Hydrogen-Isotope Electron Capture Differential Cross Sections at Small Scattering Angles," *Bull. Am. Phys. Soc.* **28**, 940 (1983).

15. J. T. Park, D. M. Blankenship, T. J. Kvale, J. L. Peacher, E. Redd, and E. Rille, "Elastic Differential Cross Sections for Proton Scattering by Atomic Hydrogen," **Proceedings of XIII International Conference on the Physics of Electronic and Atomic Collisions** (Abstracts of Contributed Papers, J. Eichler, W. Fritsch, I. V. Hertel, N. Stolterfoht, and U. Wille, Eds.), p. 350 (1983).

16. E. Rille, J. L. Peacher, T. J. Kvale, E. Redd, D. M. Blankenship, D. G. Seely, R. E. Olson, and J. T. Park, "Small Angle Scattering in Hydrogen-Isotope Collision Systems at Intermediate Energies," **Proceedings of Symposium on Atomic and Surface Physics (SASP '84)**.

17. T. J. Kvale, D. G. Seely, D. M. Blankenship, E. Redd, T. J. Gay, E. Rille, J. L. Peacher, and J. T. Park, "Angular Differential Cross Sections for the Excitation of 1^1S Helium to the 2^1S and 2^1P States by 25- to 100-keV Proton Impact," *Bull. Am. Phys. Soc.* **29**, 777 (1984). (Presented conference talk.)

18. T. J. Kvale, D. G. Seely, D. M. Blankenship, E. Redd, T. J. Gay, E. Rille, J. L. Peacher, and J. T. Park, "The Excitation of Helium to the n=3 Composite Level by Proton Impact," *Bull. Am. Phys. Soc.* **29**, 810 (1984). (Presented conference talk.)

19. E. Redd, D. M. Blankenship, T. J. Kvale, T. J. Gay, J. L. Peacher, and J. T. Park, "Core Excitation in Mg^+ Ion Impact of He," *Bull. Am. Phys. Soc.* **29**, 812 (1984).

20. T. J. Gay, D. M. Blankenship, D. G. Seely, T. J. Kvale, J. T. Park, J. L. Peacher, and E. Redd, "Impact Excitation of He by He^+ and H^+: Alignment of the He 2^1P State," *Bull. Am. Phys. Soc.* **29**, 817 (1984).

21. G. D. Alton, T. J. Kvale, and D. J. Pegg, "Production of Ca^- Through Double Charge Exchange with Li Vapor," ORNL Physics Division Report ORNL−6120, p. 11 (1985).

22. G. D. Alton and T. J. Kvale, "The Negative Ion Source Test Facility as a Negative Ion Atomic Physics Research Facility," ORNL Physics Division Report ORNL−6120, p. 138 (1985).

23. G. D. Alton, T. J. Kvale, R. N. Compton, D. J. Pegg, and J. S. Thompson, "Progress Toward Measurement of the Properties of Metastably Bound Negative Ions," ORNL Physics Division Report ORNL−6120, p. 139 (1985).

24. T. J. Kvale, G. D. Alton, R. N. Compton, D. J. Pegg, and J. S. Thompson, "An Experimental Investigation of the Metastable States in Beryllium Anions," **Proceedings of XIV International Conference on the Physics of Electronic and Atomic Collisions**, (Abstracts of Contributed Papers.) M. J. Coggiola, D. L. Huestis, and R. P. Saxon, Eds.), p. 415 (1985). (Presented conference poster.)

Experimental Determination of the Energy Level of $Be^-(1s^22s2p^2)^4P$

T. J. Kvale, G. D. Alton, and R. N. Compton[a]
Oak Ridge National Laboratory, Oak Ridge, Tennessee 37831

and

D. J. Pegg[b] and J. S. Thompson
The University of Tennessee, Knoxville, Tennessee 37996

(Received 11 March 1985)

We report the first experimental measurements for the energy level of a metastable state of Be^-. The ions were produced in sequential charge-exchange collisions between 50- to 60-keV Be^+ ions and lithium vapor. The center-of-mass energy of autodetaching electrons was found to be 2.53 ± 0.09 eV. This result is in good agreement with previously calculated values for the $Be^-(1s^22s2p^2)^4P$-state energy.

PACS numbers: 32.80.Dz, 35.10.Hn

In this paper, we report the observation of a peak in the Be^- autodetachment electron-energy spectrum which is a signature of the decay of a metastable beryllium negative-ion state. These measurements represent the first time that the energy level of a long-lived metastable state has been experimentally determined for negative ions of the group II*A* (alkaline-earth) elements. In fact, limited experimental information is available on the structure of any metastably bound atomic negative ion. Notable exceptions to this include He^-, which is a classic example of a spin-aligned metastable negative ion (see, e.g., Alton, Compton, and Pegg[1]), resonance studies from electron-atom scattering experiments (see, e.g., Burrow, Michejda, and Comer[2]), and Li^-, in which photon emission was observed between high-lying metastable states of the negative ion (see, e.g., Brooks *et al.*[3]). The fundamental nature of Be^- makes it of considerable experimental and theoretical interest. As early as 1966, the ion was reported[4,5] to be present in mass spectra of ions emitted from direct-extraction negative-ion sources. Since the first observation of Be^-, experimental values for production efficiencies[6] and autodetachment lifetimes[7] have been reported. In recent measurements on the autodetaching decay of Be^-, Bae and Peterson[7] have shown that the ion has at least two distinct lifetime components of $\sim 10^{-4}$ and $\sim 10^{-5}$ s.

Most theoretical studies indicate that Be^- is metastable,[8-13] although early theoretical calculations[14-16] suggest that $Be^-(1s^22s^23s)^2S$ is bound with respect to the ground state, $(1s^22s^2)^1S$, of beryllium. Recent theoretical calculations do not predict the existence of a stable Be^- state but predict the existence of two states, both metastable against autodetachment, which lie below the first ionization threshold of neutral beryllium—$Be^-(1s^22s2p^2)^4P$ which is bound with respect to $Be(1s^22s2p)^3P°$, and $Be^-(1s^22p^3)^4S°$ which is bound with respect to $Be(1s^22p^2)^3P$. The radiatively allowed $^4S° \rightarrow {}^4P$ transition is predicted to occur at either 263.8 nm (Ref. 9), 267.1 nm (Ref. 12), or 265.4 nm (Ref. 10). Radiation from this transition was searched for by Andersen[17] without success. A third metastable state, $Be^-(1s2s2p^3)^6S°$, has also been predicted.[9,12] This state, however, lies energetically outside the present experimental range [> 100 eV from $Be(1s^22s^2)^1S$]. Other Be^- ion states have also been theoretically studied. For instance, the $Be^-(1s^22s^22p)^2P$ configuration is predicted[18] to be a shape resonance; however, the lifetime of this state is too short to be studied with the present apparatus.

Theoretical calculations of the structure of negative ions are particularly difficult since the electron affinities are typically of the same magnitude as the difference in correlation energies between the atom and ion. Even so, most of the present information concerning metastable negative ions, other than He^-, has been provided by theoretical studies of open-shell excited-state negative-ion configurations. The first theoretical investigations of the structure and binding energies (electron affinities) for the group I*A* elements Li^-, Na^-, and K^- and the group II*A* elements Be^- and Mg^- were made by Weiss[8] who employed variational-superposition techniques. The Be^- ion was predicted to be bound relative to the neutral atomic $(1s^22s2p)^3P°$ state by 240 meV with the most likely configuration postulated to be $Be^-(1s^22s2p^2)^4P$. This configuration is metastable against autodetachment by spin-forbidden transitions—analogous to the $(1s2s2p)^4P°$ state of He^-.

Configuration-interaction calculations have been employed by Bunge *et al.*[9] in a search for possible bound excited negative-ion state configurations for the elements hydrogen through calcium. The results of these investigations indicate the existence of two metastable states of Be^-—the $Be^-(1s^22s2p^2)^4P$ which is bound relative to $Be(1s^22s2p)^3P$ by 285 meV, and $Be^-(1s^22p^3)^4S°$ which is bound relative to the $(1s^22p^2)^3P$ atomic state by 262 meV.

The fine and hyperfine energy separations, as well as

electron affinities of the lowest two bound states of Be^-, have been calculated by Beck and Nicolaides[10] through the use of a nonrelativistic many-body calculation. These studies indicate that $Be^-(1s^22s2p^2)^4P$ is bound by 218 meV relative to $Be(1s^22s2p)^3P^\circ$, while $Be^-(1s^22p^3)^4S^\circ$ is bound by 244 meV relative to $Be^-(1s^22p^2)^3P$. The lifetimes of the $Be^-(^4P_J)$ levels were also predicted[13] in a recent calculation.

The experimental techniques utilized for determining the energy levels of metastable Be^- are very similar to those used for the measurement[1] of the energy level of $He^-(1s2s2p)^4P^\circ$. For the present investigation, a Be^+ ion beam was post-accelerated to the chosen kinetic energy, momentum analyzed, and focused through a lithium vapor cell situated 1 m away from the electron spectrometer as shown in Fig. 1. This resulted in a time delay of $\sim 1\ \mu s$ between the Be^- production and detection of electrons ejected from the decay of Be^-. Thus only ions produced in states metastable against both autodetachment and radiation survive long enough to be experimentally studied. The positive, neutral, and negative components of particles emergent from the lithium vapor cell were separated upon entrance into the experimental chamber by an electrostatic deflector. Ions passing through the device were deflected by $\pm 10^\circ$ into a 1.5-cm-long gas cell. The purpose of the gas cell was to produce a high-pressure region for collisional stripping of electrons from the Be^- ion beam. A small aperature located in front of the gas cell served to collimate the Be^- beam prior to its passage through the gas cell and through the 160° spherical-sector electron-energy analyzer. The ion beam, after straight-line transit through the analyzer, was monitored in a shielded Faraday cup located at the rear of the spectrometer. Mutually perpendicular sets of Helmholtz coils were used to nullify the Earth's and stray magnetic fields in the vicinity of the electron spectrometer.

Electrons ejected in the forward direction following autodetachment or collisional stripping were energy analyzed by the electron spectrometer which was operated in the fixed-pass-energy mode. The collisionally detached peak served as the absolute reference for the determination of the energy of the autodetached electron peak in each spectrum. The ion beam energies were chosen sufficiently high (50, 55, and 60 keV) so that the collisionally detached electron peak could be resolved from the low-energy electron background peak centered at zero laboratory energy. Autodetached electrons ejected in the backward direction could not be resolved from this low-electron-energy "noise" peak. The electron signal from the analyzer was input to a CAMAC-based multichannel-analyzer data-acquistion system. Each channel of the multichannel analyzer corresponded to a unique electron energy, and the typical voltage increment used during these measurements was 24.24 meV.

The center-of-mass (or state) energy $E_{c.m.}$ of autodetached electrons ejected in the forward direction from a moving ion beam can be determined relative to the electrons which move at the projectile velocity (collisionally detached) by use of the small-angle kinematic expression (see Ref. 1). The resulting relation for $E_{c.m.}$ is given by

$$E_{c.m.} = [\sqrt{E_a} - \sqrt{E_c}]^2, \tag{1}$$

where E_a is the laboratory energy of the autodetaching peak and E_c is the laboratory energy of the collisional detachment peak. E_c is determined from the kinetic energy of the ion beam. By use of this procedure to determine $E_{c.m.}$ which is based on two peaks corresponding to physical events occurring in the same spectrum, errors due to contact and surface potentials are minimized and the need for precise knowledge of the spectrometer constant is avoided.

Electron energy spectra were acquired for Be^- ion

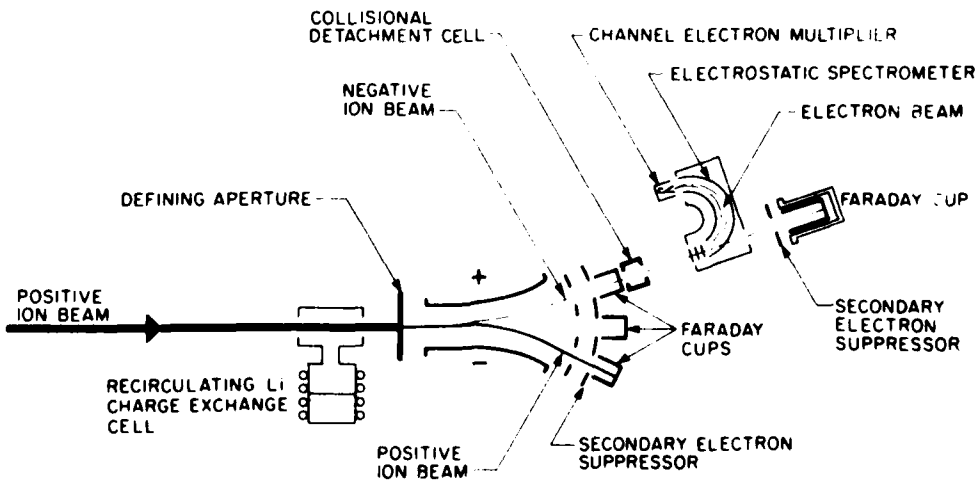

FIG. 1. The experimental arrangement used to measure the energy level of the metastable $Be^-(^4P)$ state.

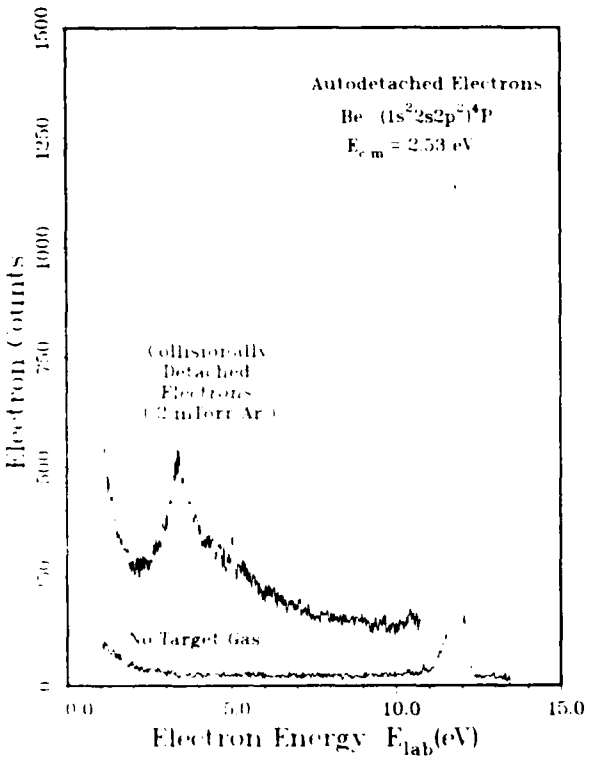

FIG. 2. Electron energy spectra from 55-keV Be^- ions with and without a thin argon target.

energies of 50, 55, and 60 keV. Figure 2 displays a high-resolution autodetachment spectrum taken without target gas and a spectrum taken with ~ 2 mTorr argon in the gas cell to enhance the collisional-detachment peak. The spectra were taken sequentially and at an ion energy of 55 keV. The very low-energy-electron background peak is attributable to low-energy electrons generated by ion impact with apertures, etc. The collisional-detachment peak was only detectable whenever a target gas (e.g., argon) was introduced into the gas cell, while the autodetachment peak was present in all of spectra. The addition of gas in the cell does not change the shape or the energy position of the autodetachment peak. This peak, which occurs at the laboratory energy of 11.71 eV for 55-keV Be^- ions, is attributable to autodetaching electrons from the decay of the $Be^-(^4P)$ state. This signal (typically several kilohertz) was well resolved from the electron background (typically < 100 Hz), while the signal-to-noise (S/N) ratio of the collisional-detachment peak was typically less than that of the autodetachment peak. The lower S/N of the collisional-detachment peak was due primarily to the higher electron background at lower electron energies. The present measurements gave an average value for the center-of-mass energy of this state measured with respect to the ground state of neutral beryllium of 2.53 eV with a standard deviation of ± 0.09 eV. The FWHM in the laboratory frame of the peak shown in Fig. 2 is ~ 0.2 eV, which corresponds to a FWHM of ~ 0.04 eV in the center-of-mass frame. From these results, we estimate an electron affinity of 195 ± 90 meV using the value from Bashkin and Stoner[19] for the energy of $Be(1s^2 2s 2p)^3P^\circ$. A search for the electron autodetachment peak from $Be^-(1s^2 2p^3)^4S^\circ$ was made without success. This is not unexpected since this state is permitted to decay radiatively to the lower-lying $Be^-(1s^2 2s 2p^2)^4P$ state.

Table I compares the present results with previous theoretical calculations. The electron affinity is defined as the energy difference between $Be(^3P^\circ)$ and $Be^-(^4P)$, whereas the energy separation between $Be(^1S)$ and $Be^-(^4P)$ is the state energy of $Be^-(^4P)$. In cases where the total energy of the ground state $Be(^1S)$ was not reported, the latest reported value by Bunge[20] was used in order to arrive at the $Be^-(^4P)$ state energy. In both cases, the resulting energy is a small difference between rather large numbers, and er-

TABLE I. Summary of experimental and theoretical values for the energy levels of the $Be^-(1s^2 2s 2p^2)^4P$ state.

Electron affinity $E(Be(^3P))$-$E(Be^-(^4P))$ (meV)	State energy $E(Be^-(4P))$ (eV)	Type	Reference
240 ± 100	2.49[a]	Theoretical	8
> 122	2.66[b]	Theoretical	12
285		Theoretical	9
217.7 ± 57.1	2.56[c]	Theoretical	10
195 ± 90[d]	2.53 ± 0.09	Experimental	Present work

[a]Used -14.6189 a.u. for the ground state of beryllium.
[b]Used -14.6684 a.u. for the ground state of beryllium, as quoted from Bunge (Ref. 20).
[c]Used -14.667328 a.u. for the ground-state energy of beryllium, as quoted from Ref. 20.
[d]Used 2.27248 eV as the state energy of $Be(1s^2 2s 2p)^3P^\circ$ taken from Ref. 19.

rors, uncertainties, or omissions are extremely important. For example, calculations (see, e.g., Ref. 8) which do not take electron correlation effects into account predict $Be^-(^4P)$ to be unbound (electron affinity $= -68$ meV). The present electron-energy measurements covered the whole region below the first ionization threshold of neutral beryllium, and only one autodetaching peak was observed in the spectrum. However, this does not conclusively rule out the existence of other metastably bound states for Be^- since our apparatus is insensitive to ions having lifetimes much less than 1 μs or much greater than a few tens of microseconds. This includes, of course, ion states that are not metastable against radiative decay.

In conclusion, the present results support the theoretical predictions that there is only one state of the negative beryllium ion lying below the $Be(1s^2 2s\,2p)^3P^\circ$ threshold which is metastable against both autodetachment and radiative decay. The agreement between the theoretically predicted electron-affinity and state-energy values and our experimentally determined values permits us to identify the observed autodetaching state as $Be^-(1s^2 2s 2p^2)^4P$. Additional support for this identification comes from lifetime predictions[13] and measurements[7] which indicate that $Be^-(^4P_J)$ will have a lifetime component matched to the time window of our apparatus.

This research was sponsored by the Division of Basic Energy Sciences, U. S. Department of Energy under Contract No. De-AC05-840R21400 with Martin Marietta Energy Systems, Inc., the U. S. Department of Navy, Office of Naval Research, Task 393-071, and the U. S. Department of Energy through the University of Tennessee under Contract No. DE-AS05-83ER13097. One of us (T.J.K.) is a postdoctoral Fellow in the U. S. Department of Energy Postgraduate Research Training Program administered by Oak Ridge Associated Universities.

[a]Also with the Department of Chemistry, University of Tennessee, Knoxville, Tenn. 37996.

[b]Also with Oak Ridge National Laboratory, Oak Ridge, Tenn. 37831.

[1]G. D. Alton, R. N. Compton, and D. J. Pegg, Phys. Rev. A **28**, 1405 (1983).

[2]P. D. Burrow, J. A. Michejda, and J. Comer, J. Phys. B **9**, 3225 (1976).

[3]R. L. Brooks, J. E. Hardis, H. G. Berry, L. J. Curtis, K. T. Cheng, and W. Ray, Phys. Rev. Lett. **45**, 1318 (1980).

[4]K. Bethge, E. Heinicke, and H. Baumann, Phys. Lett. **23**, 542 (1966).

[5]E. Heinicke, K. Bethge, and H. Baumann, Nucl. Instrum. Methods **58**, 125 (1968).

[6]J. Heinemeier and P. Hvelplund, Nucl. Instrum. Methods **148**, 65 (1978); J. Heinemeier and P. Hvelplund, Nucl. Instrum. Methods **148**, 425 (1978).

[7]Y. K. Bae and J. R. Peterson, Phys. Rev. A **30**, 2145 (1984).

[8]A. W. Weiss, Phys. Rev. **166**, 70 (1968).

[9]C. F. Bunge, M. Galán, R. Jáuregui, and A. V. Bunge, Nucl. Instrum. Methods **202**, 299 (1983).

[10]D. R. Beck and C. A. Nicolaides, Int. J. Quantum Chem. Quantum Chem. Symp. **18**, 467 (1984).

[11]C. A. Nicolaides, Y. Komninos, and D. R. Beck, Phys. Rev. A **24**, 1103 (1981).

[12]D. R. Beck, C. A. Nicolaides, and G. Aspromallis, Phys. Rev. A **24**, 3252 (1981).

[13]G. Aspromallis, C. A. Nicolaides, and D. R. Beck (to be published).

[14]R. J. Zollweg, J. Chem. Phys. **50**, 4251 (1969).

[15]H. S. W. Massey, *Negative Ions* (Cambridge Univ. Press, Cambridge, 1976).

[16]B. L. Moiseiwitsch, in *Atomic Processes and Applications*, edited by P. G. Burke and B. L. Moiseiwitsch (North-Holland, Amsterdam, 1976).

[17]T. Andersen, private communication.

[18]H. A. Kurtz and Y. Ohrn, Phys. Rev. A **19**, 43 (1979).

[19]*Atomic Energy Levels and Grotian Diagrams I: Hydrogen I–Phosphorus XV*, edited by Stanley Bashkin and John O. Stoner (North-Holland, Amsterdam, 1975).

[20]C. F. Bunge, Phys. Rev. A **14**, 1965 (1976).

Electron-detachment spectroscopy of 20—100-keV H^- projectiles interacting with thin Ar targets

G. D. Alton and R. N. Compton
Oak Ridge National Laboratory, Oak Ridge, Tennessee 37830

D. J. Pegg
Department of Physics, University of Tennessee, Knoxville, Tennessee 37916
and Oak Ridge National Laboratory, Oak Ridge, Tennessee 37830

(Received 30 July 1984)

Energy and transformed-velocity spectra of electrons emitted in the forward direction have been experimentally determined for 20–120-keV H^- projectiles traversing thin Ar targets. The spectra from H^- are surprisingly cusplike in shape even though single-electron loss is known to dominate. In contrast to the findings of Menendez and Duncan, who performed similar measurements at higher projectile velocities, target-induced structures in the electron loss to the continuum spectra are not pronounced in this velocity regime.

I. INTRODUCTION

Considerable efforts have been expended by several research groups toward elucidation of the complex physical processes of electron capture to (ECC) and loss from (ELC) continuum projectile states, both of which occur as a consequence of their traversal through thin gaseous and solid targets. These physical phenomena, though distinctly different, both exhibit themselves as sharp, cusplike peaks in the ejected-electron spectra whenever the electron velocity $\mathbf{v}_e$ matches the velocity of the ion in speed and direction. The spectral positions and similarities in shape of ECC and ELC processes make experimental distinguishability extremely difficult or impossible in cases where both processes may be present. For these reasons brief comments regarding previous studies of ECC are also included. The reader is referred to the articles by Sellin[1] and Breinig *et al.*[2] for more comprehensive reviews of previous investigations of these phenomena.

Evidence of the ECC phenomenon was first observed by Rudd *et al.*[3] in the form of enhanced doubly differential cross sections for electron ejection in the forward direction from atoms subjected to proton bombardment. Subsequent measurements by Crooks and Rudd[4] of the electron energy distributions resulting from the bombardment of He targets, also with H^+ projectiles, revealed sharp, cusplike spectra with the electron velocity at the peak of the distribution very close to that of the incident projectile. Similarly shaped peaks were also observed by Harrison and Lucas[5] in the momentum distributions of electrons emitted from thin carbon foils in the direction of the incident proton beam.

Since these early discoveries of the ECC phenomenon, many investigations have been made of the energy and momentum distributions of electrons resulting from interactions between a variety of fully stripped light and multiply charged ions interacting with thin gaseous and solid targets; all have confirmed the cusplike nature of the resulting spectra and the equivalence of the electron and projectile velocities at the peak of the distribution. In such ion-atom collisions, electrons are known to originate from capture to low-lying, projectile-centered states for bare or nearly bare energetic projectiles (ECC) and from loss to low-lying continuum states whenever loosely bound electrons are present on the projectile (ELC). Consequently, for partially stripped multiply charged ions, both processes may be present—making interpretation of the resulting spectra difficult or impossible.

The results of early theoretical approximations of the proton-induced target-electron-ejection phenomenon based on the plane-wave Born[6] and binary-encounter models[7] were found to be in good agreement with differential cross-section measurements at intermediate angles. However, at very small and large angles, significant discrepancies were observed. Thus, neither model could explain the enhanced doubly differential cross sections observed at small angles by Rudd *et al.*[3] The breakdown of these models for forward-ejected (ECC) electrons is attributable to the exclusion of long-range attractive projectile-electron interactions—a critically important requirement for explanation of this effect.[6] That is, the interaction must not only transfer momentum to the ejected electrons but must include postcollision long-range effects due to the attractive forces between the ejected electron and the positively charged projectile.[5] Several theoretical efforts have been made which take into account these final-state interactions including the works of Salin,[8] Macek,[9] Dettmann, Harrison and Lucas,[10] and Garibotti and Miraglia.[11]

The physical basis of ECC was successfully explained by Macek[9] through the use of a multiple-amplitude first-order approximation to the Faddeev integral equations with the final state for the ejected electron represented by an attractive target-centered Coulomb wave function. The theory predicts an approximately symmetric electron distribution in space at $\mathbf{v}_e \sim \mathbf{v}_i$ with a yield proportional to Z^3, where Z is the charge on the projectile. Other theoretical efforts to describe the ECC phenomenon in terms of single-amplitude first and second Born approxi-

mations have been made, including the first Born, Coulomb-distorted wave description of proton ionization of He by Salin[8] which predicts an asymmetric peak in the velocity spectrum of ejected electrons at low projectile velocities. Dettmann, Harrison, and Lucas[10] have applied the second-order Born approximation for comparison of theoretical shapes and yields of ECC spectra with those experimentally observed for H^+, H_2^+, and He^+ ions passing through thin carbon foils. The theory predicts a Z^3 yield dependence and symmetric cusp-shaped spectrum centered at $\mathbf{v}_e \sim \mathbf{v}_i$ at high projectile velocities with the full width at half maximum (FWHM) Γ increasing linearly with projectile velocity $\mathbf{v}_i$ according to $\Gamma = \frac{2}{3} v_i \theta_0$, where θ_0 is the half-angle about the direction of projectile motion. However, first-order single-amplitude theories which predict symmetric spectra for electrons emitted in the forward direction at high projectile velocities do not agree with the asymmetric character experimentally observed by Vane *et al.*[12] for fully stripped carbon and for oxygen ions interacting with Ar and by Rodbro and Andersen[13] for protons interacting with He, Ne, Ar, and H_2 targets. The asymmetric characteristics of ECC high-velocity spectra are predicted whenever higher-order terms are included in the Born expansion (Shakeshaft and Spruch[14]). Subsequent calculations by Garibotti and Miraglia[15] using the first-order term derived from a multiple scattering expansion of the I matrix also yield an asymmetric ECC (cusplike) electron distribution for electrons ejected in the forward direction.

A recent publication by Breinig *et al.*[16] summarizes the results derived from an extensive experimental research program devoted to studies of ECC and ELC near $\mathbf{v}_e \sim \mathbf{v}_i$ induced by high-energy multiply charged ions traversing thin gaseous targets and the analogous processes associated with high-energy projectiles passing through amorphous, polycrystalline, and single-crystalline targets. The paper, as well, includes a rather comprehensive review of other reported work devoted to ECC, ELC, and analogous projectile solid phenomena at high projectile velocities. The studies were made with a variety of projectiles and projectile charge states over an energy range of 0.7–8.5 MeV/u with and without coincidence requirements between the emergent charge state and forward scattered electrons. The investigations show the ECC spectra in this velocity regime to be strongly skewed toward lower velocities $\mathbf{v}_e$ while ELC in the same regime appears to be approximately symmetric with FWHM independent of $\mathbf{v}_e$. In contradistinction, the electron spectra accompanying ion penetration through solid targets in this energy range are found to be slightly skewed toward higher electron velocities while exhibiting velocity-independent widths—an assumption which is at variance with theoretical predictions. Projectile atomic-number dependence associated with the ECC differential cross section in velocity $d\sigma/dv$ for a given velocity $\mathbf{v}_e$ were found to scale according to $Z^{2.3}$ and thus substantially deviate from the Z^3 theoretical predictions of Macek[9] and Dettmann, Harrison, and Lucas.[10]

Electron loss to the continuum (ELC) occurs during projectile-target interactions whenever loosely bound electrons are present on the projectile. The ionization process exhibits itself in the form of an electron distribution, similar in shape to that of ECC with the peak centered at $\mathbf{v}_e \sim \mathbf{v}_i$. The origin of the peak can be readily visualized in terms of an energy or velocity distribution imparted to the detached electrons superposed about the centroid of the moving projectile. The underlying theoretical basis of ELC was made initially by Drepper and Briggs[18] who applied the first-order Born approximation with projectile-centered attractive Coulomb wave functions for description of projectile ionization for electrons moving in the beam direction. Briggs and Drepper,[19] in a later article, used the first Born approximation to calculate the cross section, differential in angle and velocity, for projectile-electron loss. The theory predicts a cusplike velocity distribution for electrons moving in the forward direction while electrons ejected in the backward direction are found to be adequately characterized by an elastic scattering model. The theory predicts cross sections for this process which approach constant values in the limit of $\mathbf{v}_i \gg \mathbf{v}_0$, where $\mathbf{v}_i$ is the projectile velocity and $\mathbf{v}_0$ that of the orbital velocity of the detached electron. This prediction is supported by the observed trends toward constant cross sections $d\sigma/d\Omega$ with increasing projectile velocities made by Strong and Lucas.[17] Theoretical derivations of the doubly differential ELC cross sections in the first Born plane-wave approximation have also been made by Briggs and Day[18] and Day.[19] The dependence of the cross section on small angles θ_0 with respect to the direction of the beam is derived. The FWHM of the cusp for this approximation varies according to $\Gamma = \frac{2}{3}\theta_0 v_i (1 + \frac{2}{3}\beta + \cdots)$, $-1 \leq \beta \leq 2$ where β is the anisotropy parameter which, in general, is a function of v_i. All of the theoretical estimations of ELC cross sections are valid at projectile velocities $\mathbf{v}_i \gg \mathbf{v}_0$.

The previously discussed investigations have involved the use of positive charged projectiles in measurements of ECC and ELC in laboratory observed energy or velocity distributions. The series of investigations by Menendez and Duncan[20–22] have utilized H^- projectiles in measuring ELC differential cross sections in energy and angle resulting from interactions with thin rare-gas targets and projectile energies of 0.5 and 1 MeV. These measurements are of particular relevance to the present work.

Perhaps the most interesting aspect of the work of Menendez and Duncan was the discovery of target-dependent structures in the ELC spectra near $\theta \sim 0°$ from He and Ar targets. The spectra consisted of two distinct peaks—a dominant peak centered at $\mathbf{v}_e \cong \mathbf{v}_i$ and a smaller peak displaced toward lower velocities $\mathbf{v}_e$ by ~ 30 and ~ 13.5 eV, respectively, for He and Ar targets.[21,22] The observed energy difference between the respective groups is found to be independent of H^- velocity. The discovery of unexpected spectral features associated with ELC processes has further stimulated experimental efforts and given impetus to a number of theoretical papers with the objectives of formulating a physical basis for the respective observations. Theoretical works include those of Franz, Wright, and Genoni,[23] Day,[24] Malecki and Macek,[25] and recently by Ponce and Baragiola.[26] The doubled-peaked structure is shown in the first Born approximation to be a consequence of destructive interfer-

ence between $l \sim 0$ and higher $l > 0$ partial waves or electron excitation of the target. Such structure was also predicted by Garibotti and Miraglia[27] in terms of an anticapture phenomenon for negative ions. More recently, Burgdörfer[28] has performed similar calculations which show a cusp inversion near $v_e \cong v_i$ for ELC processes in an attractive Coulomb field—the shape of which is determined not only by the final-state interaction but by dynamical effects and by symmetry of the initial state as well.

As a continuation of the previously reported studies of the spectroscopy of the metastably bound states of He^-,[29] we have measured ELC spectra near $\theta = 0°$ for H^- projectiles interacting with thin Ar targets at projectile energies between 20 and 120 keV—a region of velocity in which ELC has not been previously investigated. The principal objectives of this investigation were to study the shape and velocity dependence of electron loss spectra from H^- projectiles interacting with gaseous targets and to search for structures such as discovered by Menendez and Duncan[11,12] or collisionally induced autodetaching levels of these ions. Therefore, emphasis was not placed on measurement of absolute doubly differential cross sections.

II. EXPERIMENTAL APPARATUS AND MEASUREMENT TECHNIQUES

The details of the experimental apparatus and techniques utilized in determining the energy spectra from collisionally and autodetached H^- ions are very similar to those reported previously.[29] Negative ions were generated in a conventional duoplasmatron charge-exchange source through sequential charge-changing collisions with the exchange vapor of gaseous CH_4. The desired final energy of a particular negative-ion beam was achieved by adjusting, in combination or separately, the potentials for extraction of the positive-ion beam and post acceleration of the negative-ion beam. These potentials were accurately measured with a precision electrostatic voltmeter.

The beams were momentum analyzed and focused into a biased and shielded Faraday cup located in the experimental chamber (see Fig. 1). A small hole located in the base of the cup served as a collimating aperture (typical diameter 0.75 mm) for the beam prior to entering a ~ 1.5-cm-long gas cell, terminated by 2 mm entrance and exit apertures. The cell was used to produce a high-pressure region for collisionally detaching electrons from the respective ion beam. Target pressures were monitored with a conventional capacitance manometer. Care was taken during all measurements of electron energy spectra to ensure operation within the cell pressure range for single-collision conditions. The range for a particular ion species, detachment gas, and ion energy, was established by varying the cell pressure and noting changes in height of the detachment peaks. All pressures were then maintained within the linear pressure range established for a particular energy and detachment target.

The ion beam and detached electrons, moving collinearly with or ejected in the forward direction by autodetachment in the 5-cm drift space following the cell, enter

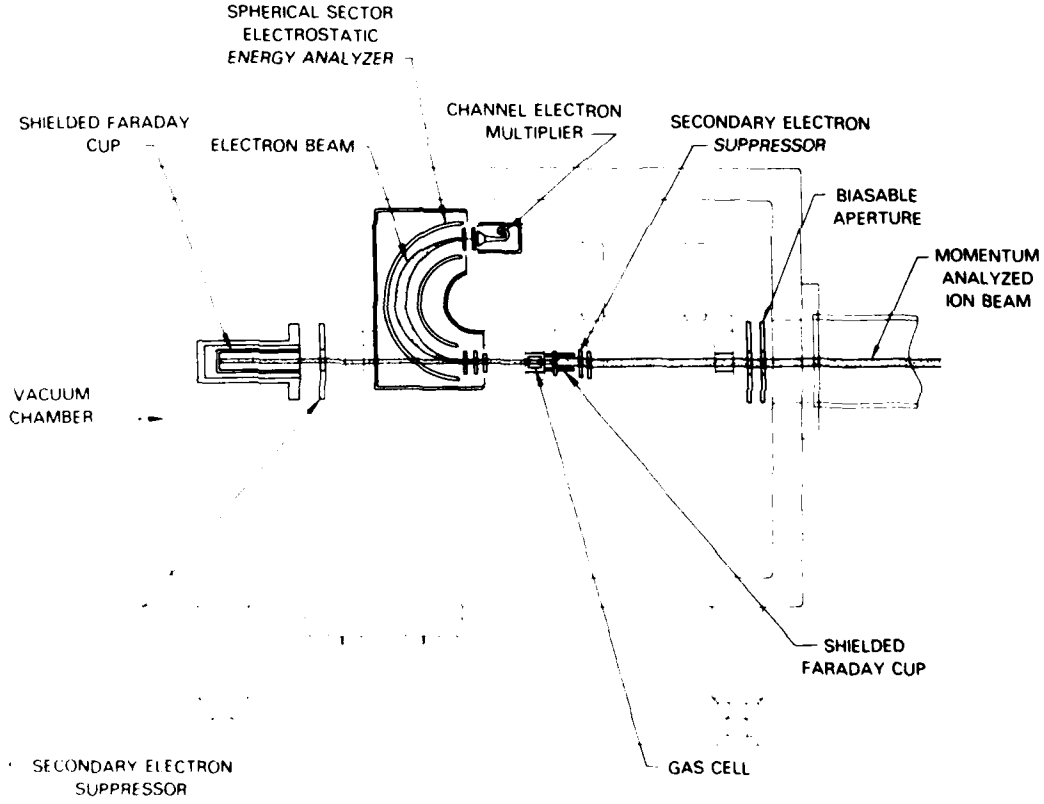

FIG. 1. Schematic drawing of the electron spectroscopy apparatus.

along the central ray into a high-resolution, double-focusing, 180°, spherical-sector, electrostatic analyzer with a mean radius of 4 cm. The ion beam passes through the spectrometer, exits through a high-transmission-gridded aperture located at the rear of the analyzer and is monitored in a shielded and biased Faraday cup. The beam collimation used in the experiments permitted angular acceptances of $\theta_0 \pm 1.5°$ with respect to the central ray of the entrance aperture of the analyzer.

During all energy-distribution measurements, the electron spectrometer was operated in a fixed pass-energy mode thus requiring the acceleration of electrons moving at energies less than and deceleration of those moving greater than the set pass energy of the analyzer. This was accomplished by linearly varying the voltage across a single-gap electrode system at the entrance of the analyzer.

The experimental chamber was equipped with three sets of mutually perpendicular Helmholtz coils which were used to nullify stray and the earth's magnetic fields in the vicinity of the electron spectrometer. This arrangement permitted the magnetic field to be reduced to ~ 1 mG over the spectrometer volume. Electron spectra were taken with a standard x-y recorder with abscissa and ordinate directions, respectively, driven by signals from a precision ramp voltage generator and a conventional channel electron-multiplier circuit. A typical count rate at the peak of the detachment signal was $\sim 10^4$ electrons/sec.

The observed laboratory energy $E_{\rm lab}$ of an electron with energy E_e and mass m_e ejected collinearly with respect to a moving ion of energy E_i and mass M_i is given by the following small-angle kinematical approximation:

$$E_{\rm lab} \cong \frac{m_e}{M_i} E_i \pm 2 \left| \frac{m_e}{M_i} E_e E_i \right|^{1/2} + E_e \ , \qquad (1)$$

where the positive and negative signs refer, respectively, to ejection of electrons in the direction of or opposite to the motion of the beam.

The center-of-mass energy E_e of autodetachment electrons ejected in the forward direction from a moving ion beam of energy E_i can be determined relative to the electrons which move at or near the projectile velocity by use of expression (1). The resulting relation for E_e is given by

$$E_e = \left| \left| \frac{m_e}{M_i} E_i + eX_i - eX_e \right|^{1/2} - \left| \frac{m_e}{M_i} E_i \right|^{1/2} \right|^2 , \qquad (2)$$

where X_i and X_e are, respectively, the potentials through which the electrons moving at or near the velocity of the ion beam and the autodetaching electrons are accelerated or decelerated upon entrance into the analyzer, and e is the electronic charge. By using this procedure, based on differences, errors due to contact and surface potentials are minimized and the need for precise knowledge of the spectrometer constant and energy-scale calibration is avoided.

III. DATA-PROCESSING PROCEDURES

Background subtraction. The spectral data, taken by use of the procedures outlined previously, were subjected to background subtraction and digitized for deconvolution from the assumed spectrometer resolution function and for velocity space transformation. The background consisted of a monotonically decreasing electron signal of low-energy electrons centered about $v_e = 0$ in the laboratory frame produced by the ion beam striking apertures situated at the entrance to the analyzer and a smaller signal which was attributable to electrons originating from the target due to direct ionization. The data shown in Fig. 2 illustrate the nature of the background spectra and are typical of those observed in these experiments. A monotonically decreasing function, similar to that shown in Fig. 2, was used to separate the ELC and low-energy electron spectra when appropriate. These data point out the difficulty associated with accurate determination of spectral shapes of the low-energy wings of the distribution at low projectile velocities. At higher projectile velocities, the two peaks become further separated and therefore the spectral shapes can be unambiguously determined. The data of Fig. 2 for H^- also show the presence of the collisionally induced autodetaching $(2s^2)^1S^e$ state of H^-. Following background subtraction, the data were digitized in preparation for deconvolution with spectrometer resolution function.

Spectra deconvolution. Various methods of deconvoluting experimentally determined data from calculated, assumed, or measured instrumental resolution functions have been described in the literature. The technique is of practical importance in that it, in principle, permits extraction of the true shapes and distributions of spectra data and enables, for example, the determination of absolute energy and transformed-velocity distributions. The result of the procedure is to accentuate structures within the data by increasing peak heights while effectively decreasing their spectral widths.

The procedures used to deconvolute data displayed in this article follow those described previously in Ref. 30 but with appropriate modifications. The observed electron-detachment rate $R(\langle \epsilon_j \rangle)$ at the jth value of the average electron energy $\langle \epsilon_j \rangle$ is an integral product of the analyzer resolution function (energy-distribution function)

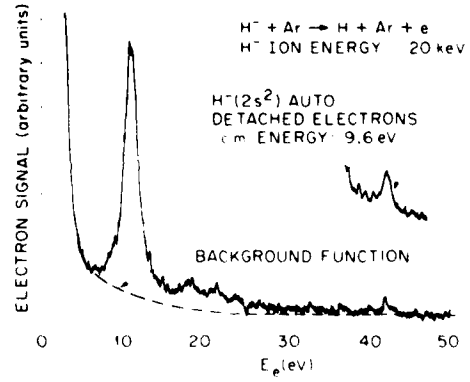

FIG. 2. Collisionally induced energy spectrum for electrons detached from 20-keV H ions interacting with Ar. The background function shown is typical of those used in data reduction for extraction of low-energy projectile-electron-detachment spectra.

$f(\langle\epsilon_j\rangle,\epsilon)$ that corresponds to the same value of the average electron energy $\langle\epsilon_j\rangle$ and $g(\epsilon)$, the monoenergetic detachment rate at energy ϵ. The observed detachment rate can, therefore, be represented according to the following expression:

$$R(\langle\epsilon_j\rangle)=\int_0^\infty g(\epsilon')f(\langle\epsilon_j\rangle,\epsilon')d\epsilon' , \tag{3}$$

where the integration extends over all ϵ'. The solution to Eq. (3) is obtained iteratively. Estimated values of $g(\epsilon)$ are introduced into Eq. (3) along with the measured or analytical energy-distribution function $f(\langle\epsilon_j\rangle,\epsilon)$ and the value $R(\langle\epsilon_j\rangle)$ is calculated for every value of $\langle\epsilon_j\rangle$ for which detachment rates have been measured. A weighting factor ω is then defined as the ratio of experimentally determined detachment rates $R_{\rm expt}$ to calculated detachment rates $R_{\rm calc}$ from the following expression:

$$\omega(\langle\epsilon_j\rangle)=R_{\rm expt}(\langle\epsilon_j\rangle)/R_{\rm calc}(\langle\epsilon_j\rangle) \tag{4}$$

with the condition that $\omega(\langle\epsilon\rangle)=1$ whenever $R_{\rm calc}(\langle\epsilon_j\rangle)=0$. The weighting factor ω is then used to define a new $g_{\rm new}(\epsilon)$ through the expression

$$g_{\rm new}(\epsilon)=g_{\rm old}(\epsilon)\sum_j\omega(\langle\epsilon_j\rangle)f(\langle\epsilon_j\rangle,\epsilon)\Big/\sum_j f(\langle\epsilon_j\rangle,\epsilon) . \tag{5}$$

Equation (3) is repeatedly solved until the residuals defined by

$$\sum_j[R_{\rm expt}(\langle\epsilon_j\rangle)-R_{\rm calc}(\langle\epsilon_j\rangle)]^2\rightarrow\text{minimum} \tag{6}$$

reach minimum values. When this condition is satisfied, the weighting factor $\omega(\langle\epsilon_j\rangle)\rightarrow 1$ and the function $g(\epsilon)$ does not change with successive iterations. The function $g(\epsilon)$ represents very nearly the absolute electron-detachment rate at energy ϵ.

The energy-distribution function $f(\langle\epsilon_j\rangle,\epsilon)$ is normalized to unity for all energies ϵ_j or

$$\int f(\langle\epsilon_j\rangle,\epsilon')d\epsilon'=1 . \tag{7}$$

The spectrometer resolution function. The resultant detachment rate $g(\epsilon)$ depends, of course, on a judicious choice of the spectrometer resolution function $f(\langle\epsilon_j\rangle,\epsilon)$. Ideally, $f(\langle\epsilon_j\rangle,\epsilon)$ should be determined experimentally by measuring the apparent energy distribution from a monoenergetic source of electrons under conditions identical to those used to obtain $R(\langle\epsilon_j\rangle)$ (defining apertures, energy, etc.), the data of interest. The resolution function used in the deconvoluted spectra displayed in this paper was determined by measurement of the energy-distribution function from the autodetaching state of (^4P)He$^-$ ($\epsilon=19.74$ eV)—a typical spectrum of which is displayed in Fig. 3. The FWHM Γ of the autodetaching electron was found to be essentially independent of He$^-$ projectile energy as shown in Fig. 4 and, therefore, the same function $f(\langle\epsilon_j\rangle,\epsilon)$ was used for deconvoluting all H$^-$ spectral data.

IV. RESULTS AND DISCUSSIONS

Electron loss to the continuum (ELC) spectral data for electrons emitted in the forward direction were measured for 20–100-keV H$^-$ projectiles interacting with thin Ar targets. Accumulated data were subjected to background subtraction, digitized, and deconvoluted from the spectrometer resolution function. A typical autodetachment electron energy spectrum resulting from the decay of the $^4P_j^o$ states of He$^-$ was used as the spectrometer resolution function for the deconvolution of all ELC data. Choice of this spectral distribution for the spectrometer resolution function is based on the near monochromaticity of the autodetaching electrons from He$^-$, the energy independence of the FWHM Γ of the observed spectra (see Fig. 4) and the fact that the spectra were determined under precisely the same experimental conditions as those existing during the measurement of the ELC spectra.

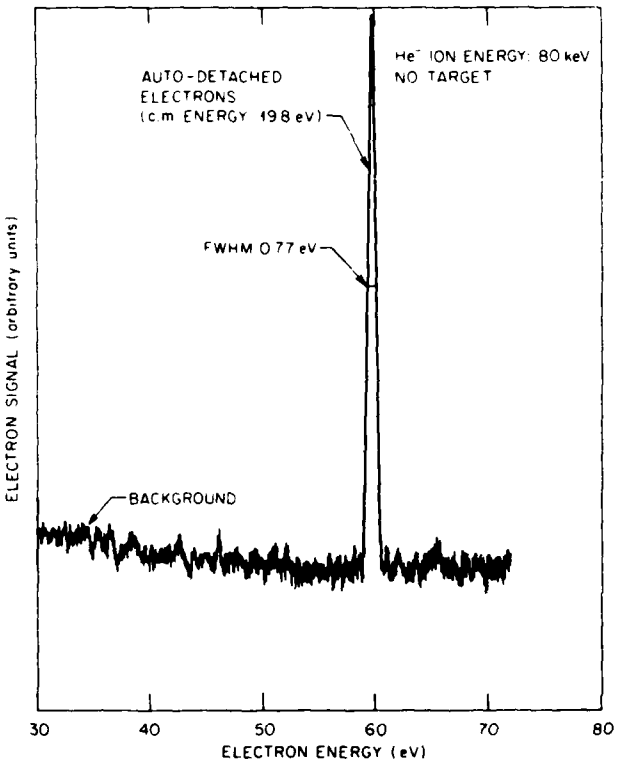

FIG. 3. Energy spectrum for electrons autodetached from 80-keV He$^-$ ions.

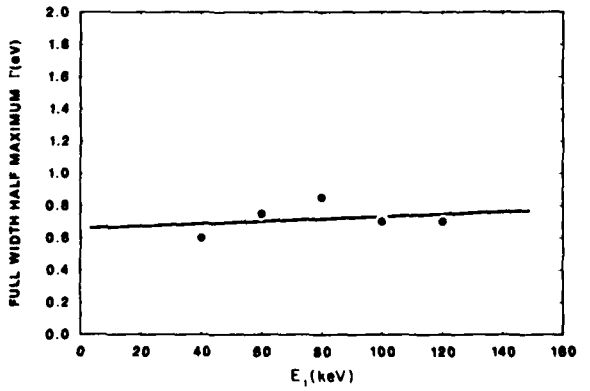

FIG. 4. Variation of the FWHM Γ of the autodetachment electron spectra from the $^4P_j^o$ state of He$^-$ with projectile energy E_i.

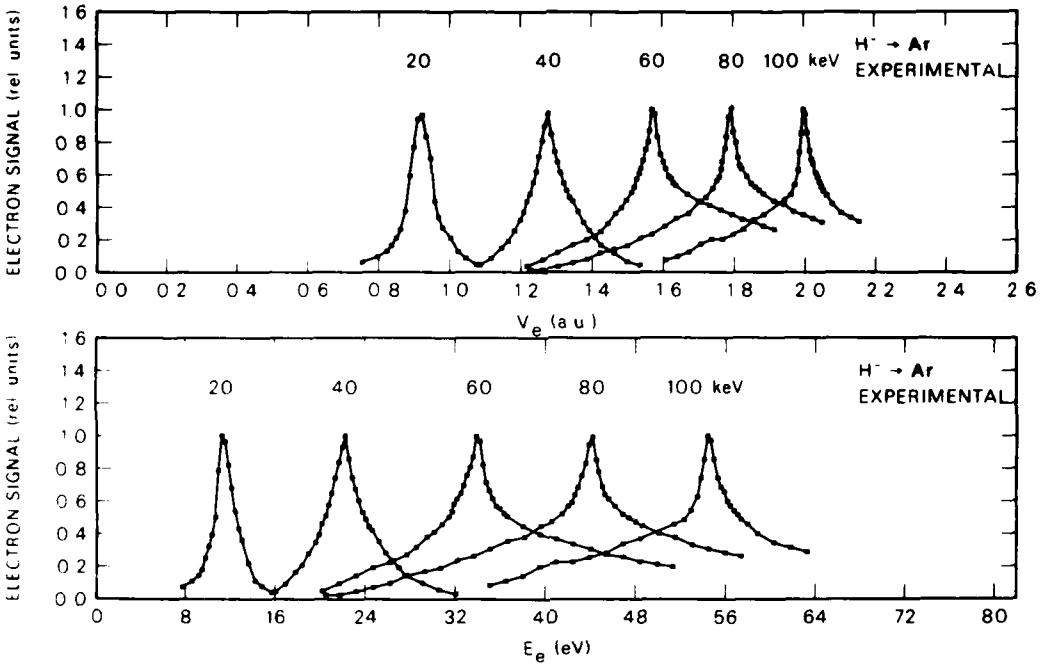

FIG. 5. Experimentally determined energy and transformed-velocity spectra for electrons detached from 20–100-keV H^- projectiles interacting with thin Ar targets. Note the appearance of structure in the low-energy side of the 100-keV spectrum.

All experimental ELC spectral data displayed in this report were normalized to unity at the maxima prior to deconvolution. The comparison deconvoluted spectra were then computed relative to the normalized experimental values. Solid lines passed through the experimental points of the spectra are added for clarity and are not least-squares fits to the data.

H^- *electron-detachment spectral data.* Collisionally induced ELC energy and velocity spectral data derived from H^- interactions with thin Ar targets are displayed in Figs. 5 and 6. Although there are no pronounced structures in these data, several aspects are worthy of comment. First of all, we note a progressive increase in the base widths of the low- and high-energy wings of these

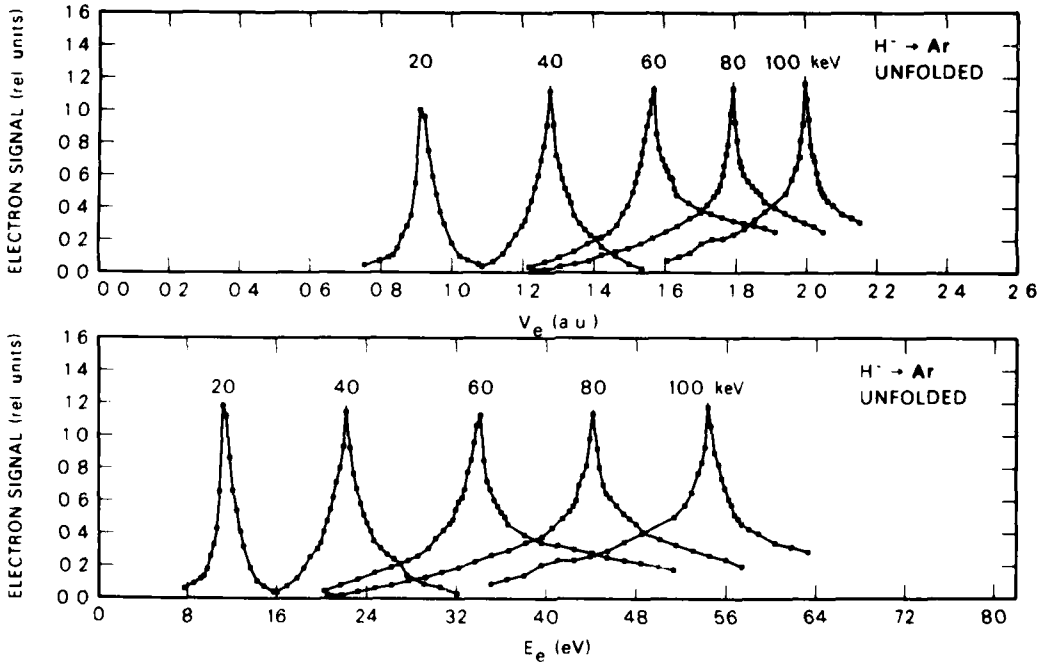

FIG. 6. Deconvoluted (unfolded) energy and transformed-velocity spectra for electrons detached from 20–100-keV H^- projectiles interacting with thin Ar targets. Note the appearance of structure on the low-energy side of the 100-keV spectrum.

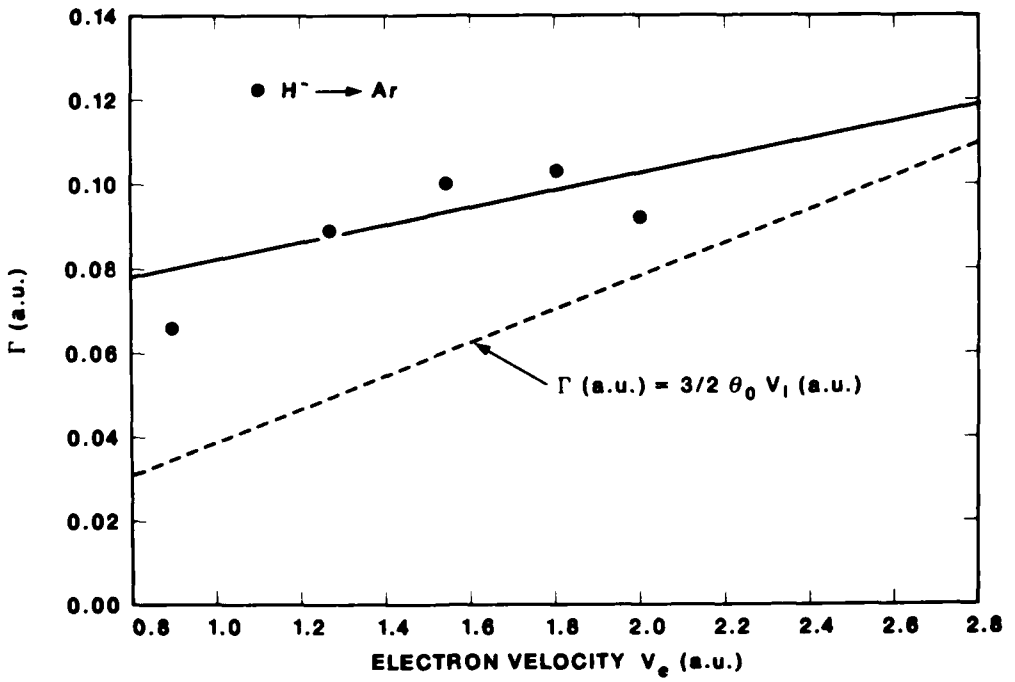

FIG. 7. Variation of the FWHM Γ with electron velocity v_e of the electron-detachment spectra of electrons ejected from 20–100-keV H^- projectiles interacting with thin Ar targets. The theoretical curve is that predicted from first Born calculations using projectile-centered Coulomb final-state wave functions.

spectra as the projectile energy increases. In addition, the spectra exhibit rather striking asymmetric cusplike characteristics in spite of the dominance of single-loss processes in this velocity regime.[31] (Single-loss cross sections are approximately an order of magnitude greater than those for double loss.[31]) While the ELC spectrum at 20 keV is symmetric, the higher-energy spectra are skewed slightly asymmetrically toward the higher electron energies. We also note a gradual appearance of structure in the low-energy wings of the 100-keV spectrum displaced with respect to the center of the ELC spectrum by ~ 13.5 eV—the position of the Ar target-dependent interference phenomena observed first by Menendez and Duncan.[21,22] The lack of such structure at lower energies is also commensurate with observed trends toward decreasing amplitudes of this phenomena with decreasing projectile energy.

The dependences of the FWHM on electron velocity are displayed in Fig. 7. The solid line represents a linear least-squares fit to the data, while the dotted line shows the theoretically predicted dependence of Γ for attractive Coulomb final-state interactions with $\Gamma = \frac{3}{2}\theta_0 v_i$. The expression is valid in the asymptotic limit of $\mathbf{v}_i \gg \mathbf{v}_0$, where $\mathbf{v}_0$ is the velocity of the electron before detachment.

V. SUMMARY AND CONCLUSIONS

Experimental investigations have been made of electron loss to the continuum (ELC) of forward-ejected electrons collisionally detached from 20–100-keV H^- projectiles during interactions with thin Ar targets. This energy range is considerably lower than has been previously investigated. The investigations reveal several interesting aspects concerning the collisionally induced electron loss to the continuum (ELC) process for H^- projectiles. The significant findings of these investigations are summarized below.

The electron energy and velocity spectra for H^- collisions with Ar targets are observed to be surprisingly cusplike in shape even though single electron-loss processes are known to dominate.[31] (The cusplike character is generally construed to be associated with attractive Coulomb final-state interactions as predicted by first-order Born approximations.) The ELC spectra for H^- are symmetric at lower ion energies and progressively become skewed for higher ion energies. The target-dependent interference phenomenon discovered by Menendez and Duncan[21,22] is depressed for energies below 100 keV where it becomes faintly observable. The FWHM Γ for H^- interacting with Ar is observed to increase in an approximately linear fashion with electron velocity.

Analogous measurements of collisionally induced projectile-electron-loss processes for other negative ions are in progress.

ACKNOWLEDGMENTS

This research was sponsored by the U.S. Department of Energy, Division of Basic Energy Sciences, under Contract No. DE-AC05-840R21400 with Martin Marietta Energy Systems, Inc., and the U.S. Department of the Navy, Office of Naval Research, Task 393-071. The authors gratefully acknowledge the assistance of Mr. Kirby Burkholder in reducing the data and Mr. Verner Anderson for the loan of the deconvolution computer program.

[1]I. A. Sellin, J. Phys. (Paris) Colloq. Suppl. No. 2, **40**, C1 (1978).
[2]M. Breinig, S. B. Elston, S. Huldt, L. Liljeby, C. R. Vane, S. D. Berry, G. A. Glass, M. Schauer, I. A. Sellin, G. D. Alton, S. Datz, S. Overbury, R. Laubert, and M. Suter, Phys. Rev. A **25**, 3015 (1982).
[3]M. E. Rudd, C. A. Sautter, and C. L. Bailey, Phys. Rev. A **3**, 1635 (1966).
[4]G. B. Crooks and M. E. Rudd, Phys. Rev. Lett. **25**, 1599 (1970).
[5]K. G. Harrison and M. W. Lucas, Phys. Lett. **33A**, 142 (1970); **35A**, 402 (1971).
[6]W. J. B. Oldham, Jr., Phys. Rev. A **140**, 1477 (1965); **161**, 1 (1967).
[7]T. F. M. Bonsen and L. Vriens, Physica (Utrecht) **47**, 307 (1970).
[8]A. Salin, J. Phys. B **2**, 631 (1969); **2**, 1225 (1969); **5**, 979 (1972).
[9]J. Macek, Phys. Rev. A **1**, 235 (1970).
[10]K. Dettmann, K. G. Harrison, and M. W. Lucas, J. Phys. B **7**, 269 (1974).
[11]C. R. Garibotti and J. E. Miraglia, Phys. Rev. A **21**, 572 (1980).
[12]C. R. Vane, I. A. Sellin, S. B. Elston, M. Suter, R. S. Thoe, G. D. Alton, S. D. Berry, and G. A. Glass, Phys. Rev. Lett. **43**, 1388 (1979).
[13]M. Rødbro and F. D. Andersen, J. Phys. B **12**, 2883 (1979).
[14]R. Shakeshaft and L. Spruch, Rev. Mod. Phys. **51**, 369 (1979); Phys. Rev. Lett. **41**, 1037 (1978).
[15]F. Drepper and J. S. Briggs, J. Phys. B **9**, 2063 (1976).
[16]J. S. Briggs and F. Drepper, J. Phys. B **11**, 4033 (1978).
[17]M. W. Lucas and R. Strong, Bull. Am. Phys. Soc. **23**, 1087 (1978).
[18]J. S. Briggs and M. H. Day, J. Phys. B **13**, 4797 (1980).
[19]M. H. Day, J. Phys. B **13**, L65 (1980).
[20]M. G. Menendez and M. M. Duncan, Phys. Rev. Lett. **40**, 1642 (1978); Phys. Rev. A **19**, 49 (1979); **23**, 1085 (1981).
[21]M. G. Menendez and M. M. Duncan, Phys. Rev. A **16**, 1799 (1977).
[22]M. G. Menendez and M. M. Duncan, Phys. Rev. A **20**, 2327 (1979).
[23]M. R. Franz, L. A. Wright, and T. C. Genoni, Phys. Rev. A **24**, 1135 (1981).
[24]M. H. Day, Phys. Rev. A **26**, 1260 (1982).
[25]N. Maleki and J. Macek, Phys. Rev. A **26**, 3198 (1982).
[26]V. H. Ponce and R. A. Baragiola, J. Phys. B **17**, 2467 (1984).
[27]C. R. Garibotti and J. E. Miraglia, J. Phys. B **14**, 863 (1981).
[28]J. Burgdörfer, Phys. Rev. Lett. **51**, 374 (1983).
[29]G. D. Alton, R. N. Compton, and D. J. Pegg, Phys. Rev. A **28**, 1405 (1983); R. N. Compton, G. D. Alton, and D. J. Pegg, J. Phys. B **13**, L651 (1980).
[30]L. G. Christorophou, D. L. McCorkle, and V. E. Anderson, J. Phys. B **4**, 1163 (1971).
[31]J. Heinemeier, P. Hvelplund, and F. R. Simpson, J. Phys. B **8**, 1880 (1975).

Photoelectron Angular Distributions for Near-Threshold Two-Photon Ionization of Cesium and Rubidium Atoms

Adila Dodhy
Physics Department, Auburn University, Auburn, Alabama 36849, and Oak Ridge National Laboratory, Oak Ridge, Tennessee 37831

and

R. N. Compton and J. A. D. Stockdale
Chemical Physics Section, Health and Safety Research Division, Oak Ridge National Laboratory, Oak Ridge, Tennessee 37831
(Received 1 October 1984)

Photoelectron angular distributions have been measured for nonresonant two-photon ionization of cesium and rubidium atoms just above the ionization threshold. The photoelectron energies ranged from 25 to 100 meV. The results are compared with theoretical estimates based on nonrelativistic atomic wave functions. Initial results are also presented for above-threshold ionization in cesium.

PACS numbers: 32.80.Fb, 32.80.Rm

Multiphoton ionization (MPI) of atoms promises new insights into various problems of atomic structure and dynamics.[1-3] Perhaps the most powerful approach is the measurement of differential cross sections,[4-10] where the angular distributions of the photoejected electrons provide data not only on the magnitudes of the transition amplitudes but also on their relative phases. In addition to providing information about the scattering phase, thus complementing single-photon studies,[11] such measurements also test our theoretical understanding of high-order bound-free transitions involving sums over virtual intermediate states.[12]

Studies of photoelectron angular distributions for alkali-metal atoms have been limited to cases of resonantly enhanced MPI[4-6,8,10] or higher-order nonresonant processes.[7,12,13] In this paper, we report photoelectron angular distributions for nonresonant two-photon ionization of cesium and rubidium atoms where the photoejected electron has an energy in the range ~ 25–100 meV. Figure 1 shows the ionization scheme for both alkali metals. The first photon lies between the $6p$ and $7p$ states for cesium and between the $5p$ and $6p$ states for rubidium.

Our measurements are novel in two respects. First, we have studied photoelectron angular distributions in a region very close to the ionization threshold. This is difficult experimentally because of the very low energy of the photoelectrons under consideration. Second, we report photoelectron angular distributions for above-threshold ionization of cesium and compare them with theoretical predictions. Such processes have been observed by others in xenon[14-18] and cesium[13] but only in higher order (order 5 in cesium and ≥ 6 in xenon).

Details of the experimental apparatus have been described recently[10] in conjunction with resonantly enhanced MPI. Briefly, the output from a Nd:YAlG (yttrium aluminum garnet) pumped dye laser (Quanta Ray, DCR-II, PDL-I) was crossed orthogonally by a thermal alkali-metal beam. The dye-laser pulse duration was 5 ns and the bandwidth was 0.02 nm. The laser was focused to a power density of 10^8 W/cm^2 by a 35-mm lens. The power density was an order of magnitude greater when electrons from above-threshold ionization were studied. The plane of polarization of the laser was rotated by a double-Fresnel rhomb. Photoelectrons emerging perpendicular to the propagation vector of the laser beam and within $\pm 2°$ were energy analyzed by a 160° spherical-sector electrostatic energy analyzer. They were then detected by

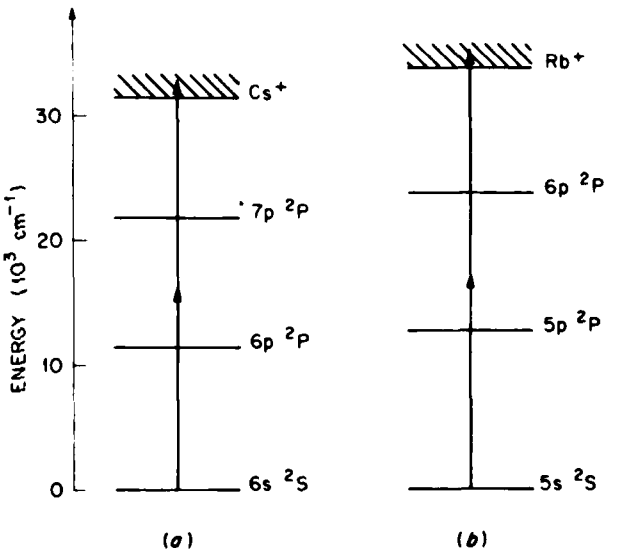

FIG. 1. Energy-level diagram showing the excitation scheme leading to ionization for nonresonant two-photon ionization of (a) cesium atoms and (b) rubidium atoms.

a dual-channelplate charged-particle detector, and the amplified signal was fed into a gated boxcar integrator (Princeton Applied Research, Model 162). Photoelectron angular distributions were obtained from a record of the relative photoelectron intensity as a function of the angle, θ, between the polarization of the laser and the fixed direction of detection of the photoelectrons. The laser–alkali-metal-atom interaction volume was carefully shielded from external electric and magnetic fields in order to detect the ultraslow photoelectrons. All critical surfaces were also coated with colloidal graphite in order to reduce surface potentials and electron reflection.

Cross sections for photoelectron angular distributions for two-photon ionization may be derived by use of time-dependent perturbation theory.[19,20] The resulting differential cross section, $\sigma(\theta)^{(2)}$, is given by

$$\sigma(\theta)^{(2)} = C^{(2)}(1+\beta_2^{(2)}\cos^2\theta+\beta_4^{(2)}\cos^4\theta), \qquad (1)$$

where $C^{(2)}$ is a normalization constant. The coefficients $\beta_l^{(2)}$ are ratios of linear combinations of second-order radial matrix elements, $r_l^{(2)}$, and cosine functions of the difference in phase shifts between the allowed $l=0$ and $l=2$ continuum waves. The radial matrix elements are given by

$$r_l^{(2)} = \sum_{np} \frac{\langle kl|r|np\rangle\langle np|r|ns\rangle}{(E_{g.s.}-E_{np}+h\omega)}, \qquad (2)$$

where $E_{g.s.}$ and E_{np} are the single-particle energies, ω is the frequency of the radiation field, k is the wave number of the photoelectron, and $\langle nl|r|nl'\rangle$ are radial dipole matrix elements. The radial wave functions for the ground states were generated in the nonrelativistic Hartree-Fock approximation. The sum over the virtual intermediate states, $|np\rangle$, found in Eq. (2) can be determined by any appropriate method. For the purposes of comparison with the experimental data, we will use the results of two independent calculations: (1) an analytic-expansion method based on a Sturmian basis set,[21–23] and (2) an inhomogeneous-differential-equation method[24–26] based on a Hartree-Fock potential.

The experimental and theoretical photoelectron angular distributions are shown in Fig. 2. The two-photon ionization threshold corresponds to a laser excitation wavelength of 636.8 nm for cesium and 593.6 nm for rubidium. The solid line through the experimental data points is the theoretical calculation using the Sturmian-basis-set method,[21] while the dashed curve is from the Hartree-Fock procedure.[24] The experimental and theoretical intensities are normalized to each other at $\theta = 0°$. Good qualitative agreement is seen between the experimental measurements and theoretical calculations for both atoms. The experimental and theoretical values for the β coefficients are shown in Table I. The experimental values were determined by least-squares fitting the data with Eq. (1). For cesium, the Sturmian procedure gives results which are actually in quite good quantitative agreement with the experimental results. In comparing the photoelectron angular distributions for the two atoms, we note that both experiment and theory find that the

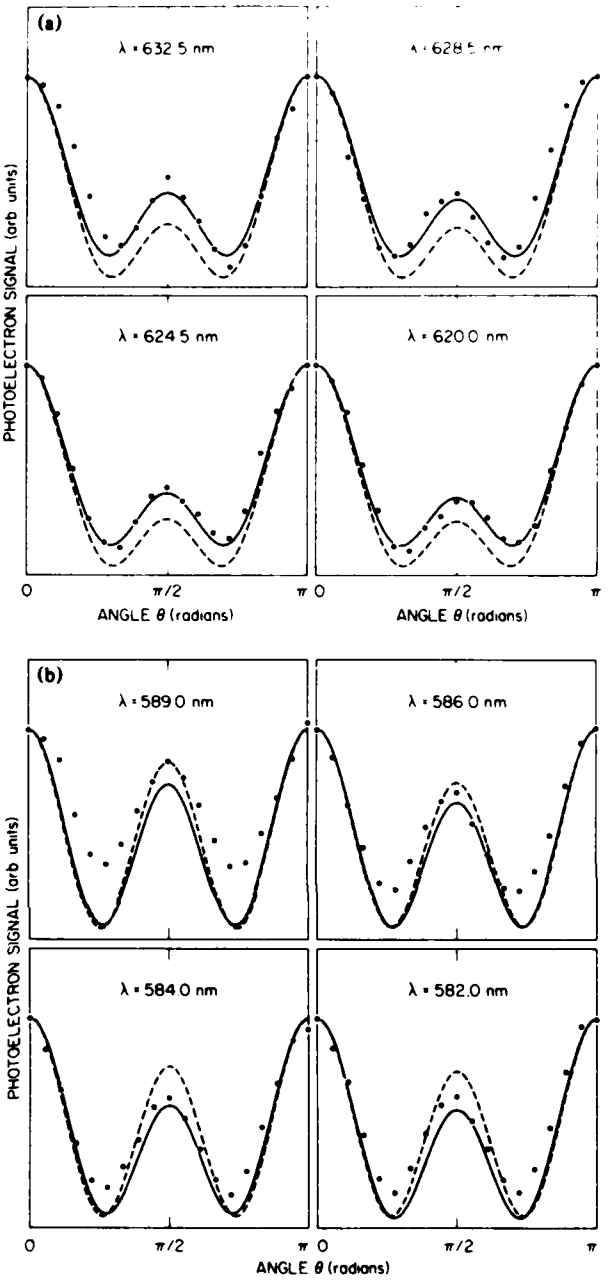

FIG. 2. Photoelectron angular distributions for nonresonant two-photon ionization of (a) cesium atoms and (b) rubidium atoms. The error bars are three times the size of the dot. The solid lines are the theoretical calculations using the Sturmian-basis-set method and the dashed curves are from the Hartree-Fock procedure.

TABLE I. Experimental and theoretical values of the β coefficients.

Alkali metals	λ (nm)	Photoelectron energy (eV)	Experiment β_2	Experiment β_4	Sturmian method β_2	Sturmian method β_4	Hartree-Fock method β_2	Hartree-Fock method β_4
Cesium	632.5	0.027	−3.18	4.42	−3.58	4.82	−4.99	7.35
	628.5	0.052	−3.29	4.78	−3.61	5.02	−5.08	7.65
	624.5	0.077	−3.29	4.87	−3.64	5.21	−5.14	7.90
	620.0	0.106	−3.55	5.43	−3.66	5.38	−5.22	8.16
Rubidium	589.0	0.033	−2.48	2.69	−3.69	4.32	−3.93	4.11
	586.0	0.055	−3.03	3.49	−4.11	4.65	−3.99	4.33
	584.0	0.069	−3.29	3.88	−4.15	4.87	−3.98	4.28
	582.0	0.084	−3.31	3.95	−4.32	5.09	−4.01	4.34

ratio of the intensity at $\theta = 90°$ to that at $\theta = 0°$ is larger in rubidium than in cesium for approximately the same value of photoelectron energy above the two-photon ionization threshold. We also note that in both atoms, this ratio decreases as the laser wavelength is decreased. The deviation of the data from the theory for photon energies nearest the threshold may be due to the difficulties with detection of ultraslow electrons or possibly due to neglect of electron correlation and relativistic effects in the calculations.

For the three-photon ionization of cesium, involving above-threshold ionization, a third photon is absorbed in the continuum. The differential cross section, $\sigma(\theta)^{(3)}$, is given by[19]

$$\sigma(\theta)^{(3)} = C^{(3)}(\cos^2\theta + \beta_4^{(3)}\cos^4\theta + \beta_6^{(3)}\cos^6\theta), \tag{3}$$

where $C^{(3)}$ is a normalization constant. The coefficients, $\beta_l^{(3)}$, are ratios of linear combinations of third-order matrix elements, $r_l^{(3)}$, and cosine functions of the difference in phase shifts between $l = 1$ and $l = 3$ continuum waves. For comparison with experiment we will again use the results of calculations which employed the Sturmian basis set[21] and Hartree-Fock procedures[24] in calculating the summation over intermediate virtual states.

The experimental and theoretical angular distributions obtained at a laser wavelength of $\lambda = 633.66$ nm are shown in Fig. 3. Both theoretical methods gave essentially identical results. The intensities are normalized at $\theta = 0°$. At $\theta = 0°$ the photoelectron peak corresponding to the three-photon above-threshold ionization was $\sim 1\%$ of that for the two-photon process. Four- and five-photon peaks were not detected. If present, their intensity is less than one-tenth that of the three-photon peak.

The measured angular distribution for the above-threshold ionization does not compare well with the theoretical calculations. The major discrepancy appears at $\theta = \pi/2$ where theory predicts zero intensity for any nonresonant multiphoton process involving an odd number of photons. It is important to note that Leuchs and Smith[7] have also observed a nonzero intensity at $\theta = \pi/2$ for five-photon nonresonant ionization of sodium. In our case, the nearest resonant intermediate state ($5d\,^2D$) is over 1000 cm^{-1} away from the first photon so that detuning far exceeds the spin-orbit coupling and the laser power is far too weak to allow for level shifting in and out of resonance. In addition, the polarization, P, of the laser was measured to be 0.99 at the laser focus. It is possible that space-charge and/or nonzero background effects coupled

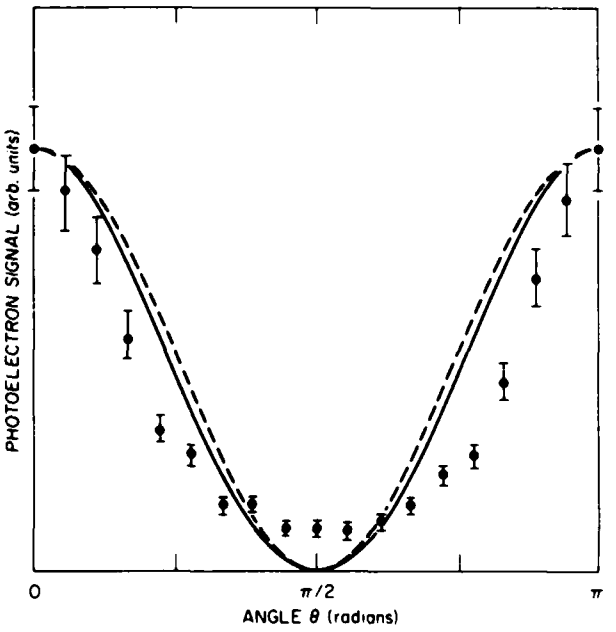

FIG. 3. Photoelectron angular distribution for above-threshold ionization in cesium at a laser excitation wavelength of 633.66 nm. The dots are the experimental values. The solid line is the theoretical calculation using the Sturmian-basis-set method and the dashed curve is from the Hartree-Fock procedure.

with the low signal level could partly account for the nonzero intensity at $\theta = \pi/2$. We note that the theory predicts primarily a $\cos^2\theta$ distribution whereas the experimental distribution contains contributions from higher-order terms. Further experimental and theoretical studies are in progress.

We wish to thank P. Lambropoulos and X. Tang of the University of Southern California and the University of Crete, and M. S. Pindzola of Auburn University for numerous helpful discussions and permission to include the theoretical calculations. This research was sponsored jointly by the Office of Health and Environmental Research, U. S. Department of Energy, under Contract No. DE-AC05-84OR21400, with Martin Marietta Energy Systems Inc., and the office of Naval Research, under Interagency Agreement No. N00014-85-F-0011.

[1]P. Lambropoulos, in *Advances in Atomic and Molecular Physics*, edited by D. R. Bates (Academic, New York, 1976), Vol. 12, pp. 87–164.

[2]*Multiphoton Processes*, edited by J. H. Eberly and P. Lambropoulos (Wiley, New York, 1978).

[3]*Multiphoton Ionization of Atoms*, edited by S. L. Chin and P. Lambropoulos (Academic, New York, 1984).

[4]J. A. Duncanson, Jr., M. P. Strand, A. Lindgrard, and R. S. Berry, Phys. Rev. Lett. **37**, 987 (1976).

[5]J. C. Hansen, J. A. Duncanson, Jr., R. L. Chien, and R. S. Berry, Phys. Rev. A **21**, 222 (1980).

[6]H. Kaminski, J. Kessler, and K. J. Kollath, Phys. Rev. Lett. **45**, 1161 (1980).

[7]G. Leuchs and S. J. Smith, J. Phys. B **15**, 1051 (1982).

[8]D. Feldmann and K. Welge, J. Phys. B **15**, 1651 (1982).

[9]R. Hippler, H.-J. Humpert, H. Schwier, S. Jetzke, and H. O. Lutz, J. Phys. B **16**, L713 (1983).

[10]R. N. Compton, J. A. D. Stockdale, C. D. Cooper, X. Tang, and P. Lambropoulos, Phys. Rev. A **30**, 1766 (1984).

[11]S. T. Manson and A. F. Starace, Rev. Mod. Phys. **54**, 389 (1982).

[12]J. Morellec, D. Normand, and G. Petite, in *Advances in Atomic and Molecular Physics*, edited by D. R. Bates (Academic, New York, 1982), Vol. 18, pp. 97–164.

[13]G. Petite, F. Fabre, P. Agostini, M. Crance, and M. Aymar, Phys. Rev. A **29**, 2677 (1984).

[14]P. Agostini, F. Fabre, G. Mainfray, G. Petite, and N. K. Rahman, Phys. Rev. Lett. **42**, 1127 (1979).

[15]P. Kruit, J. Kimman, and M. J. van der Wiel, J. Phys. B **14**, L597 (1981).

[16]F. Fabre, P. Agostini, G. Petite, and M. Clement, J. Phys. B **14**, L677 (1981).

[17]P. Kruit, H. G. Muller, J. Kimman, and M. J. van der Wiel, J. Phys. B **16**, 2359 (1983).

[18]P. Kruit, J. Kimman, H. G. Muller, and M. J. van der Wiel, Phys. Rev. A **28**, 248 (1983).

[19]P. Lambropoulos, Phys. Rev. Lett. **28**, 585 (1972).

[20]J. Mizuno, J. Phys. B **6**, 314 (1973).

[21]X. Tang and P. Lambropoulos, to be published.

[22]S. Klarsfeld and A. Maquet, J. Phys. B **12**, L553 (1979).

[23]E. Karule, J. Phys. B **11**, 441 (1978).

[24]M. S. Pindzola, private communication.

[25]M. S. Pindzola, Phys. Rev. A **17**, 1021 (1978).

[26]M. Aymar and M. Crance, J. Phys. B **14**, 3583 (1981).

THE PRODUCTION OF Ca^- THROUGH SEQUENTIAL CHARGE EXCHANGE WITH Li VAPOR*

G. D. Alton, T. J. Kvale,‡ and R. N. Compton‡‡

Oak Ridge National Laboratory
Oak Ridge, Tennessee 37831

D. J. Pegg‡‡ and J. S. Thompson‡‡‡

University of Tennessee
Knoxville, Tennessee 37916

The efficiencies for producing Ca^- through sequential charge exchange between Ca^+ projectiles and Li vapor have been measured for the first time. The measurements were made over a projectile energy range of 20 to 100 keV under experimental conditions commensurate with tandem accelerator applications. Production efficiencies in terms of negative ion charge state fractions versus projectile energy, Li vapor cell temperature and Li target density were determined for negative ion formation within a detection window α of $\pm$ 11 mrad. Within this range of angular divergence, the efficiency for production is observed to be an increasing function of the projectile energy even at the highest energies used during the measurements (100 keV). The results of these measurements as well as a description of the experimental apparatus and techniques utilized are presented.

---

*Research sponsored by the Division of Basic Energy Sciences, U.S. Department of Energy, under contract DE-AC05-840R21400 with Martin Marietta Energy Systems, Inc. and DE-AS05-83ER13097 with the University of Tennessee and the U.S. Department of the Navy, Office of Naval Research, TASK 393-071.

‡Postdoctoral Fellow in the Postgraduate Training Program administered by Oak Ridge Associated Universities, Oak Ridge, TN.

‡‡University of Tennesse, Knoxville, TN and Oak Ridge National Laboratory, Oak Ridge, TN.

‡‡‡Graduate student at the University of Tennessee, Knoxville, TN.

1. Introduction

The tandem accelerator concept is predicated on the existence of negative ions. Thus, techniques for formation of intense negative ion beams for a wide variety of elements are of considerable importance to tandem accelerator based atomic and nuclear physics research programs. In addition to these traditional applications, an increasing number of other applications have also evolved over the past few years.[1,2]

Negative ion formation through sequential charge exchange interactions between an initially positive energetic ion and a suitably chosen exchange vapor offers perhaps the most universal and efficient means of producing negative ions known to date. Production efficencies depend primarily on ion energy, the electron affinity of the element under consideration, and the electron binding energy and density of the exchange vapor. The efficiency of the exchange process depends strongly on the choice of the projectile-target combination, with highest efficiencies occurring for combinations with minimum energy defect in both of the electron capture processes.

In general, negative ion formation, for a projectile y and an exchange vapor x, takes place according to the following spin conserving interactions.

$$\begin{aligned} y^+ + x &\rightarrow y^{0*} + x^+ \\ y^{0*} + x &\rightarrow y^{*-} + x^+ \end{aligned} \qquad (1)$$

where the asterisk indicates the possibility of an excited state of the atom or ion.

The sequential electron capture process was first discovered experimentally by Donnally and Thoeming[3] in the formation of He^- in Cs vapor. Subsequently, several other investigations have been made of the efficiency and energy dependence of charge exchange production of H^- in Na[4] and Cs vapors[5] and He^- in Li, Na and Mg,[6] K,[7] Rb[8] and Cs[9] vapors. In recent years, a series of systematic investigations has been reported for the production of several negative ions in Na and Mg exchange vapors with efficiencies ranging from 0.4% to greater than 90% depending on the electron affinity of the particular element.[10,11] These investigations also include production efficiency measurements for Be^- in Na(3%)[11] and Mg (1.75%)[10] vapors and Ca^- in Na (0.4%)[11] vapor at a single energy (50 keV). These Group IIA elements have negative electron affinities and are known or believed to exist in doubly excited, metastably bound states. (Recent experimental evidence has confirmed the metastability of Be^-.)[12] Since the formation of Ca^- through charge exchange is the subject of the present study, the result for Ca^- in reference 11 is of particular relevance. The Group IIA elements are examples of a class of elements that are well suited for charge exchange negative ion production since they are difficult to produce by other means — provided, of course, that they can be formed in states which live long enough to be of practical value.

In addition to the practical utility of Ca^- ion beams for traditional tandem accelerator applications, there is considerable interest in the atomic structure properties of this negative ion as well as other members of the Group IIA elements because they are believed to be formed in doubly excited, spin-aligned states and may be metastably bound.[13] Thus, the formation of useful intensities of Ca^- could be of considerable importance for fundamental atomic physics experiments designed to determine the structure and lifetime of the ion. The present studies were motivated by the need for useful intensities of Ca^- for both tandem accelerator and fundamental atomic physics applications. The objectives of the present investigation were to determine production efficiencies for Ca^- formation in Li vapor over a projectile energy range which has not been investigated previously and to provide information for practical application of the charge exchange technique.

2. Experimental Apparatus

The Oak Ridge National Laboratory Negative Ion Source Test Facility[14] was modified in order to perform the intended charge exchange efficiency measurements. The principal components which make up the facility are illustrated schematically in Fig. 1. The pre-momentum analysis portion of the facility is composed of a universal charge exchange ion source, an einzel lens for refocusing the ion beam when the pre-momentum analysis recirculating Li cell is used for negative ion generation, adjustable object

slits for the momentum analyzer, and a cylindrical lens chamber which also houses a pre-momentum analysis Faraday cup.

The magnetic mass analysis system is equipped with rotatable pole tips so that the system can be operated with single or double focusing properties. The double focusing mode of operation was used throughout these measurements in order to optimally transport a circularly symmetric beam to the experimental apparatus. The post-momentum analysis section of the facility is equipped with a Faraday cup located at the image plane of the mass analyzer, a lens for focusing the ion beam through the post-momentum analysis recirculating Li vapor cell, and the experimental chamber which houses the deflection and monitoring equipment used to measure negative ion production efficiencies.

The universal charge exchange ion source is comprised of a hollow cathode positive ion source, an ion extractor, an einzel lens and a recirculating-type Li vapor cell. The hollow cathode ion source is operated for the generation and acceleration of positive ions which can be sequentially charge-exchanged to produce negative ions prior to or following momentum analysis. For the measurements described in this report, the post-momentum charge exchange cell was always used. In this case, singly charged positive ions produced in the hollow cathode positive source were accelerated to energies up to 100 keV prior to momentum analysis.

The momentum analyzed positive ion beam was focused through the Li recirculating charge-exchange cell situated 0.85 m in front of the experimental chamber. The close proximity of the cell to the experimental chamber permitted study of relatively short-lived bound negative-ion states.

The charge exchange cell is a commercial version of the cell described in Reference 15. The lithium oven consists of a copper-clad stainless steel reservoir with two wick-lined stainless steel tubes welded into the sides through which the beam passes. A 0.79 cm diameter, 8.25 cm long tube defines the beam interaction region. Copper is used on the reservoir to maintain a uniform (isothermal) oven temperature. Independently controlled heating elements are located on the ends of the stainless steel tubes. The heaters are used to regulate the temperature to a value suitable for the condensation of lithium (~ 300°C). The wick serves to return the condensed vapors to the reservoir. The reservoir and tube ends are maintained at set temperature values by means of a thermocouple-sensor feedback-control power supply system.

The Li vapor pressure was calculated by use of the following relation taken from the compilations of Nesmeyanov[16] where P is the pressure in Torr and T the temperature in °K

$$\text{Log}_{10}P(\text{Torr}) = 12.2992 - 8442.53/T - 1.64038 \log_{10} T + 2.599 \times 10^{-4} T. \quad (2)$$

It should be pointed out that equation 2 was determined from an ensemble of experimental vapor pressure data with a corresponding statistical scatter in values and therefore some uncertainty in the value of the vapor pressure calculated by use of the equation is to be expected.

The number density, ρ, of Li vapor was subsequently calculated by using Loschmidt's number corrected for temperature and vapor pressure according to the following relation:

$$\rho = \frac{273°K}{T(°K)} \cdot \frac{P(Torr)}{760(Torr)} \cdot 2.68719 \times 10^{19}(cm^{-3}) \qquad (3)$$

3. Experimental Procedures and Techniques

Elemental calcium metal was vaporized in a boron nitride oven connected to the plasma discharge region of the hollow cathode ion source. Helium was used to stablize the plasma discharge and to reduce any possible production of CaH^+ during the measurements. The Ca^+ ion beam was extracted by a 10- to 20-kV potential difference applied to the ion source and post-accelerated to the final kinetic energy by a linearly-graded accelerator tube prior to momentum analysis by a 90° double focusing magnet. A shielded and biased Faraday cup located after the magnet was used to monitor the Ca^+ ion beam. An $^{40}A^+$ beam was used to calibrate the mass analysis system prior to loading the oven with calcium metal. The momentum analyzed beam was focused through the Li vapor cell by means of a conventional einzel lens and directed through a limiting aperture situated in front of the experimental chamber. This arrangement defined the emergent beam

detection window to a half angle, $\alpha = \pm 11$ mrad. While this angle appears to be rather restrictive, typically 47% of the positive ion beam monitored in the post momentum analysis Faraday cup could be transported from the exit of the magnet through the room temperature Li vapor cell and into the shielded and biased Faraday cup located within the experimental chamber.

The experimental apparatus used to determine charge state fractions (production efficiencies) is shown in Fig. 2. (The charge state fraction for the production of Ca^- is used synonomously with negative ion production efficiency throughout the manuscript.) The positive, negative and neutral beams emerging from the Li vapor cell and entering the experimental chamber were separated according to charge with a computationally designed charge state analyzer system. The ion beams were deflected through $\pm 10°$ with respect to the incident beam direction into shielded and biased Faraday cups where they were monitored.

The temperature of the Li charge exchange cell was varied in order to obtain Ca^- charge state fraction data as a function of the Li areal target density $n = \rho\ell$ at each impact energy where ℓ is the length of the vapor cell and ρ has been previously defined. In computing ρ, the assumption is made that the density is uniformly distibuted over the interaction region of the cell defined previously. The charge state fraction f_j of the j^{th} beam component was calculated according to the following relation

$$f_j\,(n) = \frac{I_{+1}(1)\,(0)}{I_{+1}(1)(n)} \cdot \frac{I_j(2)(n)}{I_{+1}(2)(0)} \times 100\ (\%) \qquad j = -1, +1, +2 \qquad (4)$$

where $I^{(1)}$ and $I^{(2)}$ refer to Ca^+ ion currents measured prior to (post-momentum analysis Faraday cup) or following the Li vapor cell (experimental chamber Faraday cup), respectively. The subscript j refers to the charge state of the measured ion beam. The ion current for j = 2 is divided by 2 to obtain the particle current. This procedure tends to compensate for beam fluctuations which might occur during a particular measurement. The present experimental arrangement did not permit measurement of the neutral beam fraction.

4. Production Efficiencies

The Ca^-, Ca^{++}, and Ca^+ charge state fractions f_j are shown in Fig. 3 as functions of the Li cell temperature and in Fig. 4 as a function of the areal density, $n = \rho\ell$. The data shown in Fig. 4 were taken at 80 keV and are representative of those observed over the energy range investigated. The solid curves, again, are polynomial fits to the data points. The neutral fraction (dashed curve) was not measured, but was estimated by subtracting the Ca^+, Ca^-, and Ca^{++} fractions from 100%.

The energy dependence of the Ca^- charge state fraction f is shown in Fig. 5. The individual data points are averaged results from several individual runs at each energy. The solid curve is a polynomial fit to the data.

5. Discussions and Conclusions

There are two principal potential sources of systematic errors associated with the efficiency measurements: (1) multiple scattering of the Ca^+ ion beam by the Li target out of the detector acceptance window

($\alpha = \pm$ 11 mrad) and (2) the expected finite lifetime of the Ca^- negative ion state. Of the two, multiple scattering is expected to introduce the greatest error. Each of these effects will be discussed below.

In the present experiments, individual beam components are monitored after passing through the exchange cell and the respective beam fraction obtained by normalizing to the transmitted beam with no Li vapor in the cell. Particles which suffer violent collisions in the target may be scattered out of the detection window used in these experiments. The scattering angle will be charge state dependent, i.e., the Ca^{++} component is expected to be scattered through wider angles during formation than those associated with electron capture processes because of the smaller impact parameter required to produce the multiply charged ion. The measured charge state component will therefore be underestimated if the multiple scattering angular divergence exceeds the experimental window of detection.

In order to examine the effects of scattering on the present results, the angular scattering half widths $\alpha_{1/2}$, defined by the half width of the scattered beam at half maximum in intensity, were estimated by application of the Sigmund-Winterbon multiple scattering theory[17] or Ca^+ projectiles interacting with a Li vapor target as a function of projectile energy and target thickness. For the optimum cell temperature of 625°C, these calculations show that $\alpha_{1/2}$ is 5.8 mrad for a projectile energy of 20 keV with 50% of the beam contained within a half angle α of ~ 25 mrad and for a projectile energy of 100 keV, $\alpha_{1/2}$ is 1.2 mrad with 50% of the beam contained within an angular divergence half angle α of ~ 5 mrad. Thus, we see that

multiple scattering effects are more pronounced at the lower energies used in these experiments while at the higher energies the effect is of lesser importance. Since multiple scattering effects increase according to $(\rho\ell)^{2.5}$ and tend to dominate target atomic number effects,[18] the importance of operating the cell at the optimum temperature value, or preferably slightly below, is readily apparent. The efficiency measurements made at target densities greater than the optimum value ($n = \rho\ell = 8.2 \times 10^{15} cm^2$) are expected to be strongly affected by multiple scattering and therefore may be lower than would be realized with a larger detection solid angle. However, negative ions, due to relatively weak binding energies, are not expected to be produced in violent collisions or survive subsequent violent collisions after formation. Therefore, losses attributable to scattering outside the detection window in these experiments may not be as great as one would expect from multiple scattering calculations. Future experiments are planned which will be designed to study negative ion production efficiencies as a function of scattering angle.

Ca^- is predicted to have a negative electron affinity and therefore, a finite lifetime characteristic of a metastable state. Thus, production efficiencies at the point of detection will be lower than those at the point of production. The Li charge exchange cell is located ~ 85 cm from the Faraday cup used for detection. The velocity of the Ca^- beam ranged from 3.10×10^7 cm/s at 20 keV to 6.94×10^7 cm/s at 100 keV with a corresponding spread in transit time from the production cell to the

Faraday cup used for detection of 2.74 to 1.20 μs. Thus, the population of a metastable ion state with a lifetime of 10 μs would be reduced at the point of detection by 24% for 20 keV ion beams and by 11% for 100 keV ion beams. (An estimate of 10^{-5} for the lifetime of Ca^- was made by Heinicke et al.[19] based on the transit time between the points of generation and detection in their experimental apparatus.) Lifetime measurement experiments will be performed in the near future. An independent experiment was performed to search for autodetached electrons from Ca^-. These preliminary results indicate that Ca^- may be formed in a very long-lived state. If this is true, lifetime effects will not appreciably influence the results of these measurements.

In conclusion, we have made first measurements of the efficiency for production of Ca^- in Li vapor over an energy range never before investigated under conditions which approximate those used in tandem accelerator applications. These measurements provide data useful in practical application of the technique — and point out directions for future experiments. Future experiments are planned which will examine the negative ion production efficiencies as a function of scattering angle.

References

[1] G. D. Alton, "Ionization Phenomena and Sources of Ions," pp. 44-178 in Applied Atomic Collision Physics, H.S.W. Massey, E.W. McDaniel, and B. Bederson, Chapter 2, Vol. 4: Condensed Matter, Academic Press, Orlando, Florida, 1983.

[2] G. D. Alton, "Ionization Phenomena and Sources of Negative Ions," p. 85 in Vol. I, Proceedings, International Ion Beam Engineering Congress, Kyoto, Japan, September 12-16, 1983.

[3] B. L. Donnally and G. Thoeming, Phys. Rev. 159 (1967) 87.

[4] G. I. Dimov and G. V. Roslyakov, Instr. Expl. Tech. 17 (1974) 658.

[5] R. J. Girnius, C. J. Anderson, and L. W. Anderson, Phys. Rev. A16 (1977) 2225.

[6] B. A. D'Yachkov and V. I. Zinenko, Sov. Phys. — Tech. Phys. 16 (1971) 305.

[7] R. M. Ennis, Jr., D. E. Schechter, G. Thoeming, D. B. Schlafke, and B. L. Donnally, IEEE Trans. Nucl. Sci. NS-14 (1967) 75.

[8] R. J. Girnius and L. W. Anderson, Nucl. Instrum. Methods 137 (1976) 373.

[9] A. S. Schlacter, D. H. Loyd, P. J. Bjorkholm, L. W. Anderson, and W. Haeberli, Phys. Rev. 174 (1968) 201.

[10] J. Heinemeier and P. Hvelplund, Nucl. Instrum. Methods 148 (1975) 65.

[11] J. Heinemeier and P. Hvelplund, Nucl. Instrum. Methods 148 (1975) 415.

[12] T. J. Kvale, G. D. Alton, R. N. Compton, D. J. Pegg, and J. S. Thompson (submitted to Phys. Rev. Lett.).

[13] C. F. Bunge, M. Galan, R. Jaurequi, and A. V. Bunge, Nucl. Instrum. Methods 202 (1982) 299.

[14] ORNL Physics Division Annual Progress Report (1974),ORNL-5025, p. 192.

[15] T.J.L. Greenway, Oxford University Report 85/77 (1977).

[16] A. N. Nesmeyanov, in Vapour pressure of the chemical elements (ed. J. I. Carasso; Academic Press, New York, 1963).

[17] P. Sigmund and K. B. Winterbon, Nucl. Instrum. Methods 119 (1974) 541.

[18] J. Heinemeier, Ph.D. Dissertation, University of Aarhus, Aarhus, Denmark, 1977.

[19] E. Heinicke, H. Kaiser, R. Rackwitz, and D. Feldman, Phys. Lett. 50A, (1974) 265.

Figure captions

Fig. 1. Schematic drawing of the negative ion source test facility.

Fig. 2. Experimental arrangement for measuring production efficiencies of negative ions formed through sequential charge exchange interactions.

Fig. 3. Dependence of the measured Ca^- negative ion charge state fraction f on Li vapor cell temperature at several Ca^+ projectile energies. Cell length: 8.25 cm; cell diameter: 0.79 cm.

Fig. 4. An example of the variation of measured charge state fractions f with Li target area density $n = \rho\ell$. Ca^+ ion energy: 80 keV; Li cell temperature optimized at 625°C.

Fig. 5. Measured Ca^- negative ion charge state fractions f as a function of Ca^+ projectile energy. Li cell temperature optimized at 625°C.

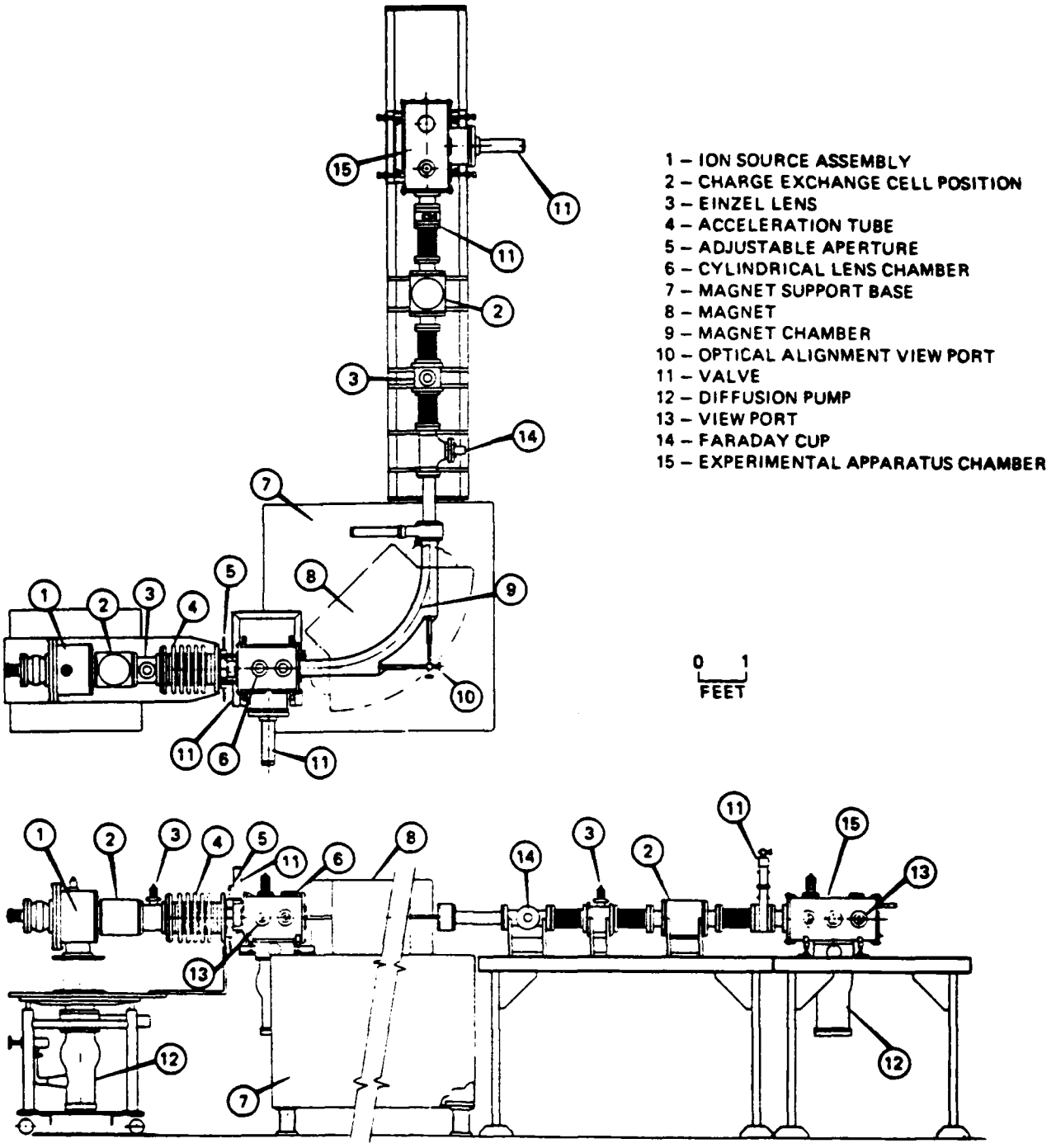
1 – ION SOURCE ASSEMBLY
2 – CHARGE EXCHANGE CELL POSITION
3 – EINZEL LENS
4 – ACCELERATION TUBE
5 – ADJUSTABLE APERTURE
6 – CYLINDRICAL LENS CHAMBER
7 – MAGNET SUPPORT BASE
8 – MAGNET
9 – MAGNET CHAMBER
10 – OPTICAL ALIGNMENT VIEW PORT
11 – VALVE
12 – DIFFUSION PUMP
13 – VIEW PORT
14 – FARADAY CUP
15 – EXPERIMENTAL APPARATUS CHAMBER
0 1
FEET

ORNL-DWG 83-16715R2

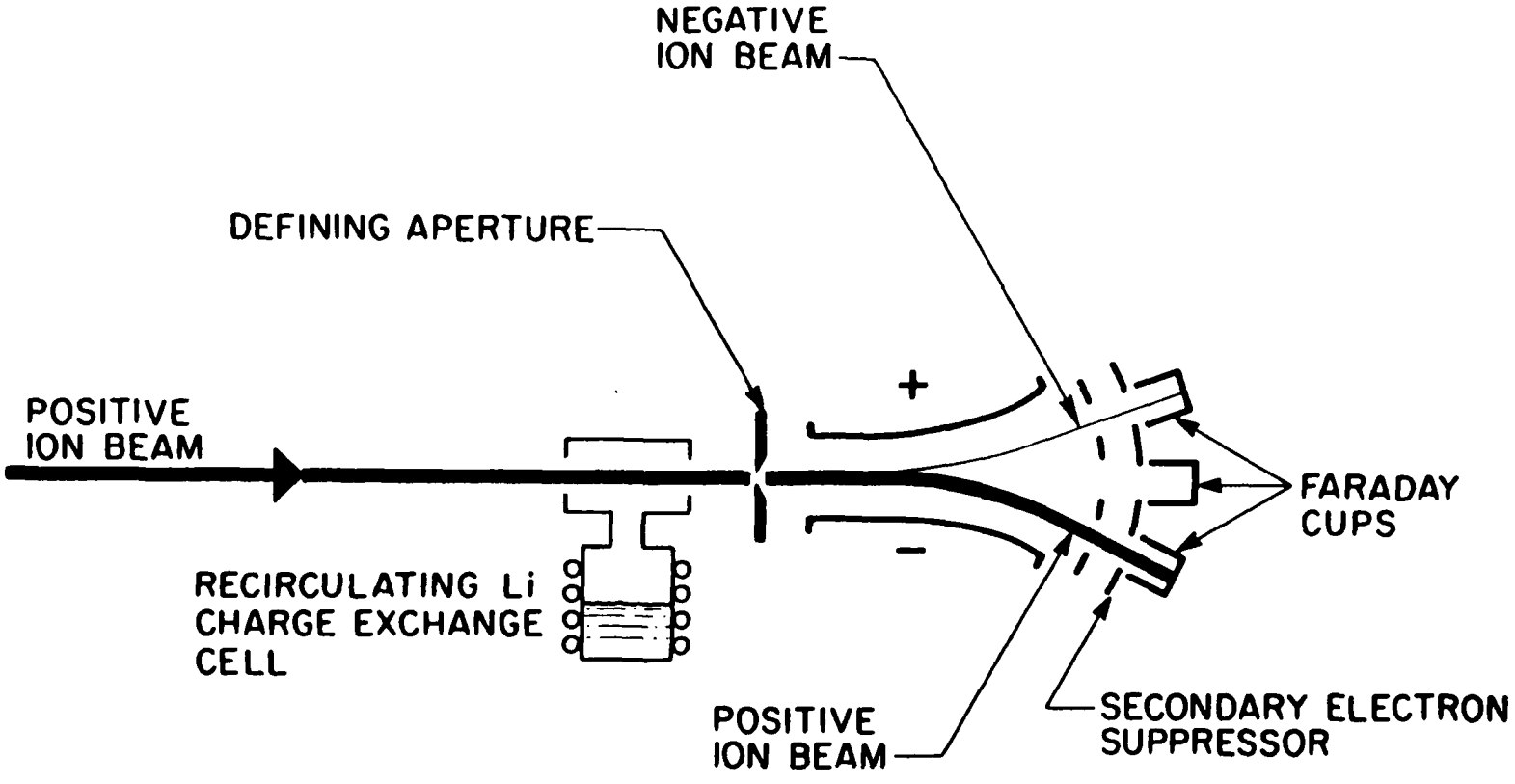

ORNL-DWG 84-16101

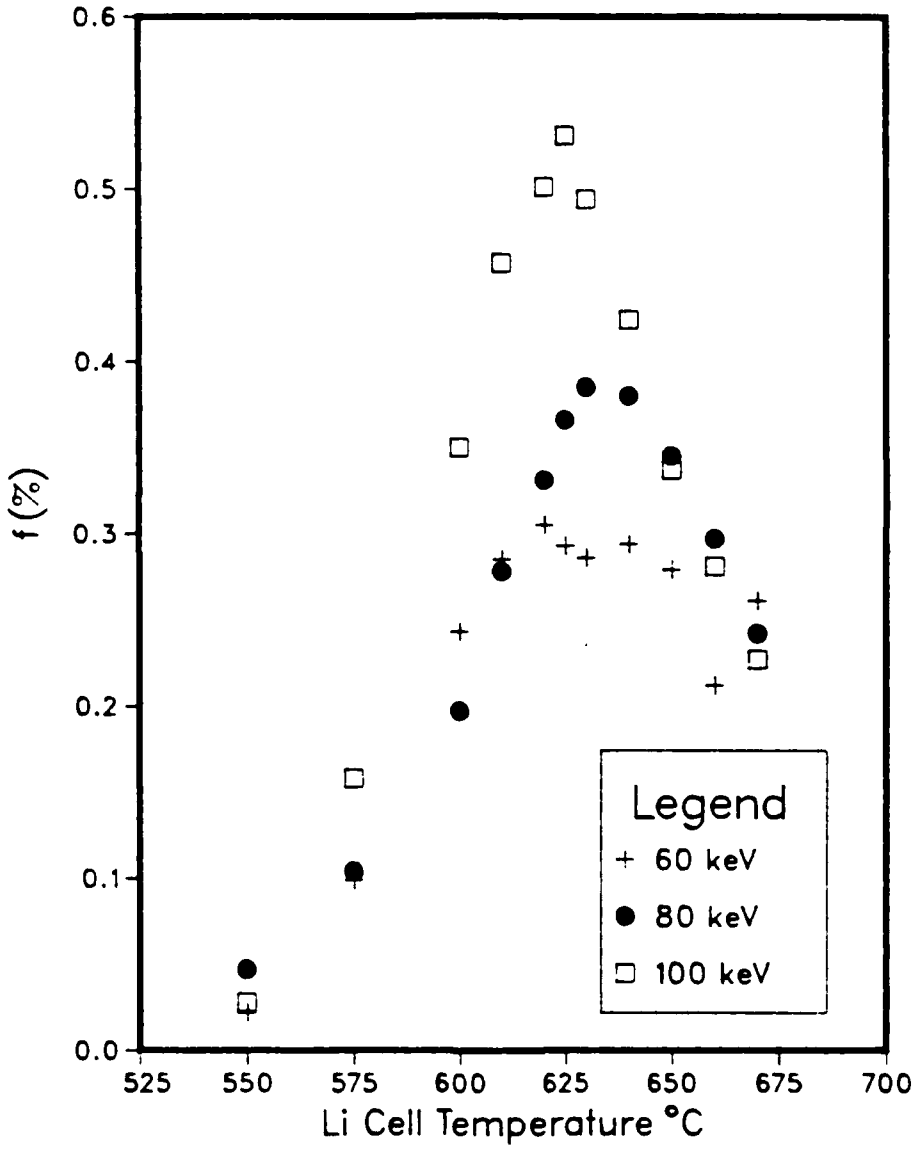

ORNL-DWG 85-9487

$Ca^+ + Li$

80 keV

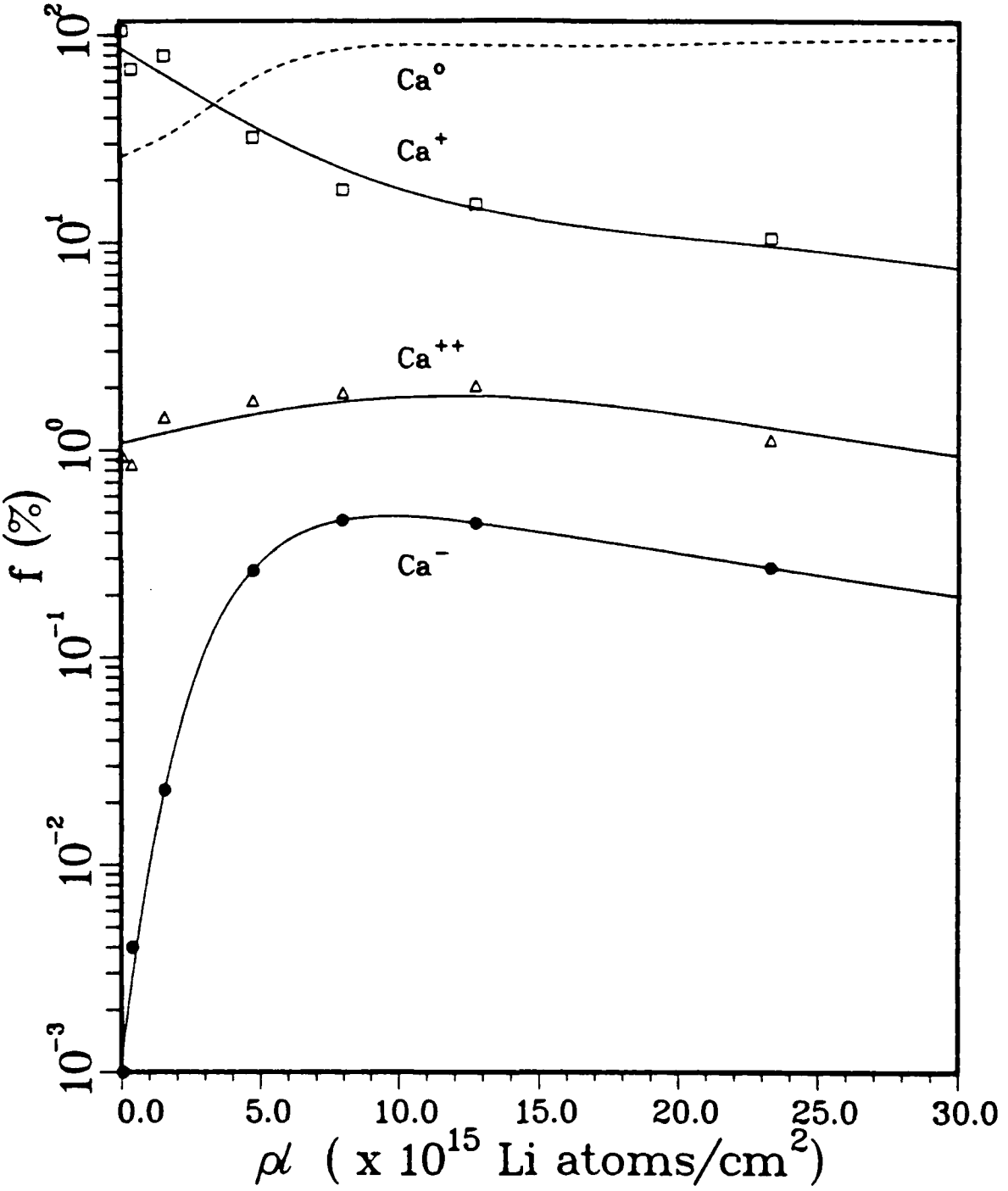

ORNL-DWG 85-9534